JINR E2-99-236

Phenomenological analysis of ε'/ε within an effective chiral lagrangian approach at $O(p^6)$

A.A.Bel'kov[1*], G.Bohm[2†], A.V.Lanyov[1‡], A.A.Moshkin[1§]

[1] Particle Physics Laboratory, Joint Institute for Nuclear Research,

141980 Dubna, Moscow region, Russia

[2] DESY – Zeuthen, Platanenallee 6, D-15735 Zeuthen, Germany

Abstract

We have combined a new systematic calculation of mesonic matrix elements at $O(p^6)$ from an effective chiral lagrangian approach with Wilson coefficients taken from [1], derived in the framework of perturbative QCD, and restricted partly by experimental data. We derive complete expressions for $K \to 2\pi$ amplitudes and compare the results for ε'/ε with experiment.

*E-mail: belkov@cv.jinr.dubna.su

†E-mail: bohm@ifh.de

‡E-mail: lanyov@mail.desy.de

§E-mail: andrem@cv.jinr.dubna.su

1 Introduction

The starting point for most calculations of nonleptonic kaon decays is an effective weak lagrangian of the form [2, 3]

$$\mathcal{L}_w^q(|\Delta S| = 1) = \sqrt{2}\, G_F\, V_{ud} V_{us}^* \sum_i C_i\, \mathcal{O}_i \tag{1}$$

which can be derived with the help of the Wilson operator product expansion from elementary quark processes, with additional gluon exchanges. In the framework of perturbative QCD the coefficients C_i are to be understood as scale and renormalization scheme dependent functions. There exist extensive next-to-leading order (NLO) calculations [4, 5] in the context of kaon decays, among others. These calculations are based on the possibility of factorization of short- and long-distance contributions into Wilson coefficient functions C_i and mesonic matrix elements of four-quark operators $\mathcal{O}_i$, respectively. The latter, however, can presently be obtained only by using non-perturbative, i.e. model-dependent, methods, because not only perturbative QCD breaks down at scales $\mu \leq 1$GeV, but also the QCD degrees of freedom (quarks and gluons) have to be replaced by the mesonic ones. Thus, a fully satisfactory solution would include the theoretical understanding of confinement. The only consistent approach to this problem may be found in lattice calculations. A discussion of the present status has been given in [6] and will not be repeated here.

Usually, the results of calculations are displayed with the help of B-factors in the form

$$T_{K\to 2\pi} = \sqrt{2}\, G_F\, V_{ud} V_{us}^* \sum_i \Big[C_i(\mu) B_i(\mu)\Big] < \pi\pi|\mathcal{O}_i|K >_{vac.sat.}\,, \tag{2}$$

where the mesonic matrix elements of four-quark operators are approximated by their vacuum saturation values, which are real and μ-independent. In principle, factors $B_i(\mu)$ should be estimated by some higher-order calculations in the long-distance regime, for instance, in $1/N_c$-expansion [7] in the form $1 + O(1/N_c)$, or from the lattice approach. The preliminary stage of these calculations is best characterized by the long standing difficulties to explain quantitatively the well-known $\Delta I = 1/2$ rule. Of course, the lack of such calculations for long-distance effects severely restricts the predictive power of (1), leaving only the possibility for some semi-phenomenological treatment [4, 1, 8], with correspondingly large theoretical uncertainties.

The main aim of the present paper is a further semiphenomenological treatment of the long-distance (non-perturbative) aspects of the above lagrangian, especially

in view of the actuality of the task to analyze the implications of the measured parameter of direct CP violation, ε'/ε. The features distinguishing our approach from others [4, 5, 9, 10, 11, 12] are mainly the following:
– At first, a chiral lagrangian up to $O(p^8)$ is used for deriving mesonic currents and densities, from which the matrix elements up to $O(p^6)$ are constructed.
– At second, according to Weinberg's power counting scheme [13], the calculation includes tree level, one- and two-loop diagrams, whereby the renormalization of the perturbative (loop) expansion for the matrix elements in question makes use of superpropagator regularization (to be discussed below), being connected to the intrinsic scale $4\pi F_0$ of the chiral lagrangian, and showing good stability (decreasing higher order contributions).
While the consistency of this approach could be checked phenomenologically in the strong interaction (hadronic) sector, in the application to the weak $\Delta S = 1$ interactions there remains the above problem of matching the scale- and scheme dependence of the C_i, thereby bridging the gap between short and long distance treatments.

In the present paper, we perform the calculation of matrix elements successively for increasing orders in p^2, displaying also the intermediate results, in order to analyze the trend of the successive expansion terms. An obstacle to this procedure is the proliferation of structure constants in higher order chiral lagrangians, which have to be fixed by experiment. This has been accomplished up to now only to $O(p^4)$ [14, 15, 16]. As a way out, we invoke another effective model – the Nambu-Jona-Lasinio (NJL) model [17] – whose modifications have been used by several groups [18, 19, 20] to "derive" the chiral lagrangian by bosonization of the fermionic degrees of freedom, suitably adapting the free parameters to reproduce those of the chiral lagrangian. In this framework, the structure constants of higher order lagrangians can be calculated, and they are well comparable in the $O(p^4)$ case with the empirical ones. Therefore it seems justified, to estimate effects of orders beyond $O(p^4)$ by taking NJL-derived structure constants.

If we compare the predicted amplitudes (2) with experiment, it turns out that even after replacing $< \pi\pi|\mathcal{O}_i|K >_{vac.sat.}$ by higher order matrix elements there are still some correction factors needed, which we call $\widetilde{B}_i$. We restrict ourselves in this paper to the display of their ranges and correlations, especially taking into account the large value ε' obtained in the NA31 experiment [21] and confirmed recently by the KTeV [22] and NA48 [23] collaborations. As our approach to the renormalization of chiral perturbation theory involves no arbitrary cut-off or scale other than F_0,

the bare π/K decay constant, there is also no other possibility to match the scale dependence of the Wilson coefficients, except that due to the renormalization of F_0 (and the other bare parameters of the effective lagrangian). This is at least partly included in our approach, as we redefine the bare coupling F_0 for each order to reach agreement with $\pi/K \to \mu\nu$ decay. As mentioned above, this procedure is stable and consistent, i.e. does not lead to large higher order corrections or large renormalization effects.

In section 2 we repeat all relevant definitions taken from our earlier work. Section 3 discusses the higher order structure constants used in the calculation of $K \to \pi\pi$ amplitudes, the latter being sketched in section 4. The last two sections give our results and conclusions.

2 Lagrangians and currents

In the present paper we use the operators $\mathcal{O}_i$ in the representation given in [2, 24]:

$$
\begin{aligned}
\mathcal{O}_1 &= \bar{u}_L\gamma_\mu u_L\;\bar{d}_L\gamma^\mu s_L - \bar{d}_L\gamma_\mu u_L\;\bar{u}_L\gamma^\mu s_L\,,\\
\mathcal{O}_2 &= \bar{u}_L\gamma_\mu u_L\;\bar{d}_L\gamma^\mu s_L + \bar{d}_L\gamma_\mu u_L\;\bar{u}_L\gamma^\mu s_L + 2\bar{d}_L\gamma_\mu d_L\;\bar{d}_L\gamma^\mu s_L + 2\bar{s}_L\gamma_\mu s_L\;\bar{d}_L\gamma^\mu s_L\,,\\
\mathcal{O}_3 &= \bar{u}_L\gamma_\mu u_L\;\bar{d}_L\gamma^\mu s_L + \bar{d}_L\gamma_\mu u_L\;\bar{u}_L\gamma^\mu s_L + 2\bar{d}_L\gamma_\mu d_L\;\bar{d}_L\gamma^\mu s_L - 3\bar{s}_L\gamma_\mu s_L\;\bar{d}_L\gamma^\mu s_L\,,\\
\mathcal{O}_4 &= \bar{u}_L\gamma_\mu u_L\;\bar{d}_L\gamma^\mu s_L + \bar{d}_L\gamma_\mu u_L\;\bar{u}_L\gamma^\mu s_L - \bar{d}_L\gamma_\mu d_L\;\bar{d}_L\gamma^\mu s_L\,,\\
\mathcal{O}_5 &= \bar{d}_L\gamma_\mu\lambda_c^a s_L\left(\sum_{q=u,d,s}\bar{q}_R\,\gamma^\mu\,\lambda_c^a\,q_R\right)\,,\quad \mathcal{O}_6 = \bar{d}_L\gamma_\mu s_L\left(\sum_{q=u,d,s}\bar{q}_R\,\gamma^\mu\,q_R\right)\,,\\
\mathcal{O}_7 &= 6\bar{d}_L\gamma_\mu s_L\left(\sum_{q=u,d,s}\bar{q}_R\,\gamma^\mu\,Q\,q_R\right)\,,\quad \mathcal{O}_8 = 6\bar{d}_L\gamma_\mu\lambda_c^a s_L\left(\sum_{q=u,d,s}\bar{q}_R\,\gamma^\mu\,\lambda_c^a\,Q\,q_R\right)\,,
\end{aligned}
$$

where $q_{L,R} = \frac{1}{2}\,(1 \mp \gamma_5)q$; λ_c^a are the generators of the $SU(N_c)$ color group; Q is the matrix of electric quark charges. The operators $\mathcal{O}_{5,6}$ containing right-handed currents are generated by gluonic penguin diagrams and the analogous operators $\mathcal{O}_{7,8}$ arise from electromagnetic penguin diagrams. The operators $\mathcal{O}_{1,2,3,5,6}$ and $\mathcal{O}_4$ describe the transitions with $\Delta I = 1/2$ and $\Delta I = 3/2$, respectively, while the operators $\mathcal{O}_{7,8}$ contribute to the transition with both $\Delta I = 1/2$ and $\Delta I = 3/2$.

The Wilson coefficients C_i of the effective weak lagrangian (1) with four-quark operators $\mathcal{O}_i$ are connected with the Wilson coefficients c_i corresponding to the basis of four-quark operators Q_i given in Refs. [1, 4], by the following linear relations:

$$
C_1 = c_1 - c_2 + c_3 - c_4 + c_9 - c_{10}\,,\quad C_2 = \frac{1}{5}(c_1 + c_2 - c_9 - c_{10}) + c_3 + c_4\,,
$$

$$C_3 = \frac{1}{5}C_4 = \frac{1}{5}\Big(\frac{2}{3}(c_1+c_2)+c_9+c_{10}\Big)\,,$$
$$C_5 = c_6\,,\quad C_6 = 2\Big(c_5+\frac{1}{3}c_6\Big)\,,\quad C_7 = \frac{1}{2}\Big(c_7+2c_8\Big)\,,\quad C_8 = \frac{1}{4}c_8\,. \tag{3}$$

The bosonized version of the effective Lagrangian (1) can be expressed in the form [25]:

$$\begin{aligned}
\mathcal{L}_w^{mes} &= \widetilde{G}_F\Big\{(-\xi_1+\xi_2+\xi_3)\Big[(J^1_{L\mu}-iJ^2_{L\mu})(J^4_{L\mu}+iJ^5_{L\mu})-(J^3_{L\mu}+\frac{1}{\sqrt{3}}J^8_{L\mu})(J^6_{L\mu}+iJ^7_{L\mu})\Big]\\
&+(\xi_1+5\,\xi_2)\sqrt{\frac{2}{3}}\,J^0_{L\mu}(J^6_{L\mu}+iJ^7_{L\mu})+\frac{10}{\sqrt{3}}\,\xi_3\,J^8_{L\mu}(J^6_{L\mu}+iJ^7_{L\mu})\\
&+\xi_4\Big[(J^1_{L\mu}-iJ^2_{L\mu})(J^4_{L\mu}+iJ^5_{L\mu})+2\,J^3_{L\mu}(J^6_{L\mu}+iJ^7_{L\mu})\Big]\\
&-4\,\xi_5\Big[(J^1_R-iJ^2_R)(J^4_L+iJ^5_L)-(J^3_R-\frac{1}{\sqrt{3}}J^8_R-\sqrt{\frac{2}{3}}\,J^0_R)(J^6_L+iJ^7_L)\\
&\quad-\sqrt{\frac{2}{3}}\,(J^6_R+iJ^7_R)(\sqrt{2}J^8_L-J^0_L)\Big]\\
&+\xi_6\sqrt{\frac{3}{2}}\,(J^4_{L\mu}+iJ^5_{L\mu})J^0_{R\mu}+6\,\xi_7\,(J^6_{L\mu}+iJ^7_{L\mu})(J^3_{R\mu}+\frac{1}{\sqrt{3}}\,J^8_{R\mu})\\
&-16\,\xi_8\Big[(J^1_R-iJ^2_R)(J^4_L+iJ^5_L)+\frac{1}{2}\,(J^3_R-\frac{1}{\sqrt{3}}J^8_R-\sqrt{\frac{2}{3}}\,J^0_R)(J^6_L+iJ^7_L)\\
&\quad+\frac{1}{\sqrt{6}}\,(J^6_R+iJ^7_R)(\sqrt{2}\,J^8_L-J^0_L)\Big]\Big\}+\text{h.c.}
\end{aligned} \tag{4}$$

Here $\widetilde{G}_F = \sqrt{2}\,G_F\,V_{ud}V^*_{us}$, $J^a_{L/R\,\mu}$ and $J^a_{L/R}$ are bosonized $(V\mp A)$ and $(S\mp P)$ meson currents and densities, corresponding to the quark currents $\bar{q}\gamma_\mu\frac{1}{4}(1\mp\gamma^5)\lambda^a q$ and densities $\bar{q}\frac{1}{4}(1\mp\gamma^5)\lambda^a q$, respectively ($\lambda^a$ are the generators of the $U(3)_F$ flavor group);

$$\xi_1 = C_1\left(1-\frac{1}{N_c}\right)\,,\qquad \xi_{2,3,4} = C_{2,3,4}\left(1+\frac{1}{N_c}\right)\,,$$
$$\xi_{5,8} = C_{5,8}\left(1-\frac{1}{N_c^2}\right)+\frac{1}{2N_c}C_{6,7}\,,\qquad \xi_{6,7} = C_{6,7}\,, \tag{5}$$

where the color factors $1/N_c$ originate from Fierz-transformations of four-quark operators $\mathcal{O}_i$ (see more technical details in [25]).

Only the even-intrinsic-parity sector of the chiral strong lagrangian is required to describe nonleptonic kaon decays up to and including $O(p^6)$. The meson currents/densities $J^a_{L/R\mu}$ and $J^a_{L/R}$ are obtained from the quark determinant by variation over additional external sources associated with corresponding quark currents and densities [25]. From the momentum expansion of the quark determinant to $O(p^{2n})$

one can derive the strong lagrangian for mesons $\mathcal{L}_{eff}$ of the same order and the corresponding currents and densities $J^a_{L/R\mu}$ and $J^a_{L/R}$ to the order $O(p^{2n-1})$ and $O(p^{2n-2})$, respectively. For example, from the terms of quark determinant of $O(p^2)$ one obtains the following:

$$\begin{aligned}
\mathcal{L}^{(p^2)}_{eff} &= -\frac{F_0^2}{4}\,\mathrm{tr}\,(L_\mu^2) + \frac{F_0^2}{4}\,\mathrm{tr}\,(\chi U^\dagger + U\chi^\dagger)\,, \\
J^{(p^1)a}_{L\mu} &= \frac{iF_0^2}{4}\,\mathrm{tr}\,(\lambda^a L_\mu)\,, \quad J^{(p^0)a}_{L} = \frac{F_0^2}{4}\overline{m}R\;\mathrm{tr}\,(\lambda^a U)\,,
\end{aligned} \tag{6}$$

where $U = \exp\left(\frac{i\sqrt{2}}{F_0}\varphi\right)$, with φ being the pseudoscalar meson matrix, and $L_\mu = D_\mu U\, U^\dagger$, $D_\mu U = \partial_\mu U + (A^L_\mu U - U A^R_\mu)$ and $A^{R/L}_\mu = V_\mu \pm A_\mu$ are right/left-handed combinations of vector and axial-vector fields. Furthermore, $F_0 \approx 90$ MeV is the bare coupling constant of pion decay, $\chi = \mathrm{diag}(\chi_u^2, \chi_d^2, \chi_s^2) = -2m_0{<}\overline{q}q{>}F_0^{-2}$ is the meson mass matrix, $\chi_u^2 = 0.0114\,\mathrm{GeV}^2$, $\chi_d^2 = 0.025\,\mathrm{GeV}^2$, $\chi_s^2 = 0.47\,\mathrm{GeV}^2$, m_0 is the current quark mass matrix, ${<}\overline{q}q{>} = (-220\mathrm{MeV})^3$ is the quark condensate, $\overline{m} \approx 265$ MeV is an average constituent quark mass, and $R = {<}\overline{q}q{>}/(\overline{m}F_0^2) = -4.96$.

At $O(p^4)$ one gets

$$\begin{aligned}
\mathcal{L}^{(p^4)}_{eff} \;\Rightarrow\; & \left(L_1 - \frac{1}{2}L_2\right)(\,\mathrm{tr}\,L_\mu^2)^2 + L_2\,\mathrm{tr}\left(\frac{1}{2}[L_\mu, L_\nu]^2 + 3(L_\mu^2)^2\right) + L_3\,\mathrm{tr}\,[(L_\mu^2)^2] \\
& -L_4\,\mathrm{tr}\,(L_\mu^2)\;\mathrm{tr}\,(\chi U^\dagger + U\chi^\dagger) - L_5\,\mathrm{tr}\left(L_\mu^2(\chi U^\dagger + U\chi^\dagger)\right) \\
& +L_8\,\mathrm{tr}\left((\chi^\dagger U)^2 + (\chi U^\dagger)^2\right) + H_2\,\mathrm{tr}\,\chi\chi^\dagger\;, \\
J^{(p^3)a}_{L\mu} \;\Rightarrow\; & i\,\mathrm{tr}\left\{\lambda^a\Big[L_4 L_\mu\,\mathrm{tr}(\chi U^\dagger + U\chi^\dagger) + \frac{1}{2}L_5\{L_\mu, (\chi U^\dagger + U\chi^\dagger)\}\Big]\right\}, \\
J^{(p^2)a}_{L} \;\Rightarrow\; & -\overline{m}R\,\mathrm{tr}\left\{\lambda^a\Big[L_4 U\,\mathrm{tr}(L_\mu^2) + L_5(L_\mu^2 U) - 2L_8 U\chi^\dagger U - H_2\chi\Big]\right\},
\end{aligned} \tag{7}$$

where L_i and H_2 are structure constants introduced by Gasser and Leutwyler [14].

For the sake of brevity, here and in the following expressions for the lagrangian at $O(p^6)$ we restrict ourselves to the terms which are necessary to calculate the decay $K \to 2\pi$. At $O(p^6)$ one needs the following terms: [1]:

$$\begin{aligned}
\mathcal{L}^{(p^6)}_{eff} \;\Rightarrow\; & \mathrm{tr}\Big\{Q_{12}\Big(\chi R^\mu U^\dagger (D_\mu D_\nu U + D_\nu D_\mu U) U^\dagger L^\nu \\
& \quad +\chi^\dagger L^\mu U(\overline{D}_\mu \overline{D}_\nu U^\dagger + \overline{D}_\nu \overline{D}_\mu U^\dagger) U R^\nu\Big) \\
& +Q_{13}\Big[\chi(\overline{D}_\mu \overline{D}_\nu U^\dagger L^\mu L^\nu + R^\nu R^\mu U \overline{D}_\mu \overline{D}_\nu U^\dagger) \\
& \quad +\chi^\dagger(D_\mu D_\nu U R^\mu R^\nu + L^\nu L^\mu D_\mu D_\nu U)\Big]
\end{aligned}$$

[1] The rather lengthy full expression for the bosonized effective lagrangian at $O(p^6)$ was presented in Refs.[20].

$$
\begin{aligned}
&+Q_{14}\Big[\chi\Big(U^\dagger D_\mu D_\nu U\overline{D}^\mu\overline{D}^\nu U^\dagger+\overline{D}_\mu\overline{D}_\nu U^\dagger D^\mu D^\nu U U^\dagger\Big)\\
&\quad+\chi^\dagger\Big(U\overline{D}_\mu\overline{D}_\nu U^\dagger D^\mu D^\nu U+D_\mu D_\nu U\overline{D}^\mu\overline{D}^\nu U^\dagger U\Big)\Big]\\
&+Q_{15}\chi^\dagger L_\mu\chi R^\mu+Q_{16}\Big(\chi^\dagger\chi R_\mu R^\mu+\chi\chi^\dagger L_\mu L^\mu\Big)\\
&+Q_{17}\Big(U\chi^\dagger U\chi^\dagger L_\mu L^\mu+U^\dagger\chi U^\dagger\chi R_\mu R^\mu\Big)+Q_{18}\Big[(\chi U^\dagger L_\mu)^2+(\chi^\dagger U R_\mu)^2\Big]\\
&+Q_{19}\Big[(\chi U^\dagger)^3+(\chi^\dagger U)^3\Big]+Q_{20}\Big(U^\dagger\chi\chi^\dagger\chi+U\chi^\dagger\chi\chi^\dagger\Big)\Big\}\,, \qquad (8)
\end{aligned}
$$

where Q_i are structure constants introduced in [20], whereas $R_\mu = U^\dagger D_\mu U$. The corresponding terms of $(V \mp A)$ and $(S \mp P)$ bosonized meson currents are given by

$$
\begin{aligned}
J_{L\mu}^{(p^5)a} \;\Rightarrow\; & i\frac{1}{4}\mathrm{tr}\Big\{\lambda^a\Big[-2Q_{14}\Big[(U\chi^\dagger+\chi U^\dagger)D_\mu D_\nu U\,U^\dagger L^\nu+D_\mu D_\nu U(U^\dagger\chi U^\dagger+\chi^\dagger)L^\nu\\
&\quad-U\overline{D}^\nu\Big((U^\dagger\chi+\chi^\dagger U)\overline{D}_\nu\overline{D}_\mu U^\dagger+\overline{D}_\nu\overline{D}_\mu U^\dagger(U\chi^\dagger+\chi U^\dagger)\Big)\\
&\quad+L^\nu U\Big((U^\dagger\chi+\chi^\dagger U)\overline{D}_\mu\overline{D}_\nu U^\dagger+\overline{D}_\mu\overline{D}_\nu U^\dagger(U\chi^\dagger+\chi U^\dagger)\Big)\\
&\quad+D^\nu\Big((U\chi^\dagger+\chi U^\dagger)D_\nu D_\mu U+D_\nu D_\mu U(U^\dagger\chi+\chi^\dagger U)\Big)U^\dagger\Big]\\
&+2Q_{15}(U\chi^\dagger L_\mu\chi U^\dagger+\chi U^\dagger L_\mu U\chi^\dagger)+2Q_{16}(\{U\chi^\dagger\chi U^\dagger,L_\mu\}+\{\chi\chi^\dagger,L_\mu\})\\
&+2Q_{17}(\{(U\chi^\dagger)^2,L_\mu\}+\{(\chi U^\dagger)^2,L_\mu\})\\
&-4Q_{18}(U\chi^\dagger L_\mu U\chi^\dagger+\chi U^\dagger L_\mu\chi U^\dagger)\Big]\Big\}\,,
\end{aligned}
$$

and

$$
\begin{aligned}
J_L^{(p^4)a} \;\Rightarrow\; & \overline{m}R\mathrm{tr}\Big\{\lambda^a\Big[Q_{12}\,L^\mu U\{\overline{D}_\mu,\overline{D}_\nu\}U^\dagger\,UR^\nu\\
&+Q_{13}(L^\nu L^\mu D_\mu D_\nu U+D_\mu D_\nu U\cdot R^\mu R^\nu)\\
&+Q_{14}(U\overline{D}^\nu\overline{D}^\mu U^\dagger D_\nu D_\mu U+D_\nu D_\mu U\overline{D}^\nu\overline{D}^\mu U^\dagger\cdot U)\\
&+Q_{15}\,L^\mu\chi R_\mu+Q_{16}\,(\chi R_\mu^2+L_\mu^2\chi)+Q_{17}(U\chi^\dagger U R_\mu^2+L_\mu^2 U\chi^\dagger U)\\
&+2Q_{18}\,L^\mu U\chi^\dagger L_\mu U+Q_{19}(U\chi^\dagger)^2U+Q_{20}(\chi U^\dagger\chi+\chi\chi^\dagger U+U\chi^\dagger\chi)\Big]\Big\}\,.
\end{aligned}
$$

We do not show explicitly the terms of the effective action at $O(p^8)$ generating the scalar current $J_L^{(p^6)}$ which is necessary for the full calculation of the tree-level matrix elements at $O(p^6)$ for the penguin operators, since the corresponding contributions turn out to be negligibly small.

3 Structure constants

For numerical estimates of $K \to 2\pi$ amplitudes and $\varepsilon^{'}/\varepsilon$ we will need the values of the structure constants L_i and Q_i which were introduced in the effective chiral

lagrangians at $O(p^4)$ and $O(p^6)$, respectively. The current experimental status of the effective chiral lagrangian at $O(p^4)$ has been discussed within ChPT in some detail in [16]. For the $O(p^4)$ lagrangian (7) all structure constants L_i are at present determined phenomenologically as measurable values L_i^r depending on the renormalization scale $\tilde{\mu}$. The best values of the parameters L_i quoted at a ρ-meson mass scale and the sources of the experimental information used are listed in table 1. The scale dependence of the measurable coefficients L_i^r is determined by relation

$$L_i^r(\mu_2) = L_i^r(\mu_1) + \frac{\Gamma_i}{(4\pi)^2}\ln\frac{\mu_1}{\mu_2}\,, \tag{9}$$

where the coefficients Γ_i are also given in table 1.

In the context of the scale dependence of the structure coefficients L_i, we have to note that in our approach the UV divergences resulting from meson loops at $O(p^4)$ and $O(p^6)$ were separated by using the superpropagator (SP) regularization method [26] which particularly well suits the treatment of loops in nonlinear chiral theories. The result is related to the dimensional regularization technique though some the difference lies in the scale parameter $\tilde{\mu}$ which is no longer arbitrary but fixed by the inherent scale of the chiral theory $\tilde{\mu} = 4\pi F_0 \approx 1$ GeV, and the UV divergences have to be replaced by a finite term using the following substitution:

$$(\mathcal{C} - 1/\varepsilon) \to C_{SP} = -1 + 4\mathcal{C} + \beta\pi\,,$$

where $\mathcal{C} = 0.577$ is Euler's constant, $\varepsilon = (4-D)/2$, and β is an arbitrary constant introduced by the Sommerfeld-Watson integral representation of the superpropagator based on unitarity.

The phenomenological analysis of the so-called Skyrme and non-Skyrme structures in the effective chiral lagrangian at $O(p^4)$ was earlier carried out in [28] by using the direct SP-calculations of meson loops for $\pi\pi$-scattering amplitudes. After reformulating this analysis in terms of the structure coefficients L_i, the values

$$L_1 = (0.6 \pm 0.2)\cdot 10^{-3}\,, \quad L_2 = (1.6 \pm 0.3)\cdot 10^{-3}\,, \quad L_3 = (-3.5 \pm 0.6)\cdot 10^{-3} \tag{10}$$

were obtained from the experimental data on $\pi\pi$-scattering lengths. In the same way, taking into account the tadpole loops, the splitting of the decay constants F_π and F_K was used at $O(p^4)$ to fix $C_{SP} \approx 3.0$ and $L_5 = (1.6 \pm 0.3)\cdot 10^{-3}$. The latter value as well as the values (10) are in a good agreement with the corresponding ones given in table 1. This fact indicates that the choice $\tilde{\mu} = m_\rho$ for the renormalization

scale of ChPT proves to be consistent with the internal scale of SP-regularization. Therefore, we use the values of L_i given in table 1 for further phenomenological analysis.

The structure constants Q_i of the $O(p^6)$ lagrangian (8) are still not defined from experiment. Therefore we need some theoretical model to estimate their values. Both the structure constants L_i and Q_i can be obtained from the modulus of the logarithm of the quark determinant of the NJL-type model [17] which explicitly contains, apart from the pseudoscalar Goldstone bosons, also scalar, vector and axial-vector resonances as dynamic degrees of freedom. However, in order to avoid double counting in calculating pseudoscalar meson amplitudes when taking into account resonance degrees of freedom, one has to integrate out (reduce) these resonances in the generating functional of the bosonization approach. As a consequence of this procedure, the structure coefficients of pseudoscalar low-energy interactions will be quite strongly modified. In this way one effectively takes into account resonance-exchange contributions [19, 27, 20].

Without reduction of resonance degrees of freedom, the structure constants $L_i = N_c/(16\pi^2)\cdot l_i$, and $Q_i = N_c/(32\pi^2\overline{m}^2)\cdot q_i$ are fixed from the bosonization of an NJL-type model as

$$
\begin{aligned}
&l_1 = \frac{1}{2}l_2 = \frac{1}{24}\,, \quad l_3 = -\frac{1}{6}\,, \quad l_4 = 0\,, \quad l_5 = xy - x\,,\\
&l_8 = \frac{1}{2}xy - x^2y - \frac{1}{24}\,,
\end{aligned}
$$

and

$$
\begin{aligned}
&q_{12} = \frac{1}{60}\,, \quad q_{13} = -\frac{1}{3}\Big(\frac{1}{20} - x + c\Big)\,, \quad q_{14} = \frac{x}{6}\,,\\
&q_{15} = \frac{2}{3}x(1-x) - \Big(\frac{1}{3} - 2x\Big)c\,, \quad q_{16} = -\frac{1}{120} + \frac{4}{3}x^2 + \frac{x}{6}(1-4x) - 2\Big(x - \frac{1}{6}\Big)c\,,\\
&q_{17} = \frac{1}{120} + \frac{x}{6}(1-4x) - \Big(x + \frac{1}{6}\Big)c\,, \quad q_{18} = \frac{4}{3}x^2 + \Big(\frac{1}{6} - x\Big)c\,,\\
&q_{19} = -\frac{1}{240} - x^2 + \frac{2}{3}x^3 + x(1+2xy)c\,,\\
&q_{20} = \frac{1}{240} + x^2 + 2(1-2y)x^3 - x(1+2xy)c\,,
\end{aligned}
$$

where $x = -\overline{m}F_0^2/(2{<}\overline{q}q{>}) = 0.1$, $y = 4\pi^2F_0^2/(N_c\overline{m}^2) = 1.5$ and $c = 1 - 1/(6y)$.

After reduction of the resonances, the structure coefficients get the form

$$
l_1^{red} = \frac{1}{2}l_2^{red} = \frac{1}{12}\Big[Z_A^8 + 2(Z_A^4 - 1)\Big(\frac{1}{4}\tilde{y}(Z_A^4 - 1) - Z_A^4\Big)\Big]\,,
$$

$$l_3^{red} = -\frac{1}{6}\Big[Z_A^8 + 3(Z_A^4-1)\Big(\frac{1}{4}\tilde{y}(Z_A^4-1) - Z_A^4\Big)\Big]\,,$$
$$l_4^{red} = 0\,, \quad l_5^{red} = (\tilde{y}-1)\frac{1}{4}Z_A^6\,, \quad l_8^{red} = \frac{\tilde{y}}{16}Z_A^4\,, \quad h_2^{red} = \tilde{y}Z_A^2\Big(\frac{Z_A^2}{8} - x\Big)\,.$$

and

$$q_{12}^{red} = q_{13}^{red} = 0\,, \quad q_{14}^{red} = \frac{1}{24}Z_A^6\,,$$
$$q_{16}^{red} = q_{17}^{red} = -\frac{Z_A^6}{64}\Big\{\tilde{y} - Z_A^2\Big[4 - 6\Big(1+4(1-Z_A^2)\Big)(1-\tilde{y}) + 4\Big(1+16(1-Z_A^2)\Big)\frac{1-\tilde{y}}{\tilde{y}}\Big]\Big\}\,,$$
$$q_{15}^{red} = -2q_{18}^{red} = \frac{1}{48}Z_A^6\Big[3\tilde{y} - 2Z_A^2\Big(5 - 12(1-Z_A^2)\frac{(1-\tilde{y})^2}{\tilde{y}}\Big)\Big]\,,$$
$$q_{19}^{red} = \frac{1}{3}q_{18}^{red} = -\frac{1}{192}Z_A^6(3\tilde{y}-2)\,,$$

where $\tilde{y} = 4\pi^2 F_0^2/(Z_A^2 N_c \overline{m}^2) = 2.4$, and $Z_A^2 = 0.62$ is the $\pi - A_1$ mixing factor.

In table 1 we also present the predictions of the NJL model for the structure coefficients L_i which after reduction of meson resonances turn out to be in a good agreement with phenomenology. This fact indicates that the NJL-model is a reasonable low-energy approximation for the effective four-quark interaction, generating a realistic effective meson lagrangian. Therefore we also use it to fix the values of the structure constants Q_i for numerical estimates of the contributions of the $O(p^6)$ lagrangian (8).

4 Amplitudes of $K \to 2\pi$ decays

Using isospin relations, the $K \to 2\pi$ decay amplitudes can be parameterized as

$$T_{K^+\to\pi^+\pi^0} = \frac{\sqrt{3}}{2}\,A_2\,,$$
$$T_{K_S^0\to\pi^+\pi^-} = \sqrt{\frac{2}{3}}\,A_0 + \frac{1}{\sqrt{3}}\,A_2\,, \qquad T_{K_S^0\to\pi^0\pi^0} = \sqrt{\frac{2}{3}}\,A_0 - \frac{2}{\sqrt{3}}\,A_2\,.$$

The isotopic amplitudes $A_{2,0}$ determine the $K \to 2\pi$ transitions into states with isospin $I = 2, 0$, respectively:

$$A_2 = a_2\, e^{i\delta_2}\,, \qquad A_0 = a_0\, e^{i\delta_0}\,,$$

where $\delta_{2,0}$ are the phases of $\pi\pi$-scattering. It is well known that direct CP violation results in an additional (small) relative phase between a_2 and a_0. Let us next introduce the contributions of the four-quark operators $\mathcal{O}_i$ to the isotopic amplitudes

$\mathcal{A}_I^{(i)}$ by the relations

$$A_I \;=\; \mathcal{F}_I\mathcal{A}_I\,, \quad \mathcal{A}_I = -i\sum_{i=1}^{8}\xi_i\mathcal{A}_I^{(i)}\,, \tag{11}$$

where $\mathcal{F}_2 = \sqrt{2}\mathcal{F}_0 = \frac{\sqrt{3}}{2}\widetilde{G}_F F_0(m_K^2 - m_\pi^2)$.

At $O(p^2)$, corresponding to the soft-pion limit, for the nonzero tree-level amplitudes $\mathcal{A}_I^{(i)}$ we obtain the following expressions:

$$\begin{aligned}
&\mathcal{A}_0^{(1)} = -\mathcal{A}_0^{(2,3)} = -\mathcal{A}_0^{(4)} = -1\,, \quad \mathcal{A}_0^{(7)} = -\mathcal{A}_2^{(7)} = 2\,, \quad \mathcal{A}_0^{(5)} = -32\Big(\frac{R\overline{m}}{F_0}\Big)^2 L_5\,,\\
&\mathcal{A}_0^{(8)} = \frac{16(R\overline{m})^2}{m_K^2 - m_\pi^2}\Big\{1 - \frac{2}{F_0^2}\Big[6L_4(\chi_s^2 + \chi_d^2 + \chi_u^2)\\
&\qquad\qquad +(L_5 - 4L_8)(\chi_s^2 + 3\chi_d^2 + 2\chi_u^2) + 2L_5 m_\pi^2\Big]\Big\}\,,\\
&\mathcal{A}_2^{(8)} = \frac{8(R\overline{m})^2}{m_K^2 - m_\pi^2}\Big\{1 - \frac{2}{F_0^2}\Big[6L_4(\chi_s^2 + \chi_d^2 + \chi_u^2)\\
&\qquad\qquad +(L_5 - 4L_8)(\chi_s^2 + 3\chi_d^2 + 2\chi_u^2) + 2L_5 m_K^2\Big]\Big\}\,.
\end{aligned} \tag{12}$$

The L_8 and H_2 contributions in the penguin operators $\mathcal{O}_{5,8}$ also have a tadpole contribution from $K \to$ (vacuum), included through strong rescattering, $K \to \pi\pi K$ with $K \to$ (vacuum). At $O(p^2)$, in case of the penguin operator $\mathcal{O}_5$, the L_8 and H_2 contributions to the direct matrix element from $K \to 2\pi$ vertices, are fully canceled by the tadpole diagrams [2]. This is due to the possibility of absorbing the tadpole contribution into a redefinition of the $K \to 2\pi$ vertex if all particles are on mass shell. Moreover, such a cancelation is expected at all orders of $K \to 2\pi$ amplitudes including loop diagrams due to general counter term arguments given in [15]. According to these arguments the structure constant H_2 is not directly measurable and does not occur in the amplitudes of physical processes.

Some interesting observations on the difference of the momentum behavior of penguin and non-penguin operators can be drawn from power-counting arguments. According to Eq. (6) the leading contributions to the vector currents and scalar densities are of $O(p^1)$ and $O(p^0)$, respectively. Since in our approach the non-penguin operators are constructed out of the products of $(V-A)$-currents $J_{L\mu}^a$, while the penguin operators are products of $(S-P)$-densities J_L^a, the lowest-order contributions of non-penguin and penguin operators are of $O(p^2)$ and $O(p^0)$, respectively. However, due to the well-known cancelation of the contribution of the gluonic penguin operator

[2] We thank W.A. Bardeen and A.J. Buras for drawing our attention to this point.

$\mathcal{O}_5$ at lowest order [29], the leading gluonic penguin as well as non-penguin contributions start from $O(p^2)$ [3]. Consequently, in order to derive the $(V-A)$-currents which contribute to the non-penguin transition operators at leading order, it is sufficient to use the terms of the quark determinant to $O(p^2)$ only. At the same time the terms of the quark determinant to $O(p^4)$ have to be kept for calculating the penguin contribution at $O(p^2)$, since it arises from the combination of $(S-P)$-densities from Eqs. (6) and (7), which are of $O(p^0)$ and $O(p^2)$, respectively. In this subtle way a difference in momentum behavior is revealed between matrix elements for these two types of weak transition operators; it manifests itself more drastically in higher-order lagrangians and currents. This fact makes penguins especially sensitive to higher order effects.

Our calculations involve Born and one- and two-loop meson diagrams and take into account isotopic symmetry breaking ($\pi^0-\eta-\eta^{'}$ mixing). The use of a specialized analytical computation package based on REDUCE [30] to calculate amplitudes and loop integration makes it possible to evaluate a large number of loop diagrams arising for different charge channels. The main problem in the calculation of amplitudes at $O(p^6)$ is the evaluation of two-loop diagrams. A part of them is shown schematically in figure 1 (we do not show rather trivial diagrams with tadpole loops). The diagrams of figure 1a were calculated analytically, because the integration in every loop can be performed independently when using the superpropagator regularization. The two-loop diagrams of figure 1b,c,d cannot be calculated analytically, but they can be estimated numerically through a dispersion-relation approach in the same way as it was already done in [31] for the so-called "box" and "acnode" diagrams. Such numerical estimates have shown that the contributions of diagrams of 1b,c,d do not exceed 2% and can be neglected.

Table 2 presents the modification of the amplitudes $\mathcal{A}_I^{(i)}$ when including successively the higher order corrections at $O(p^4)$ and $O(p^6)$. In our numerical estimates the Born contribution at $O(p^4)$ and the one-loop contribution at $O(p^6)$ were calculated for central values of the phenomenological parameters L_i from table 1. The Born contribution at $O(p^6)$ has been estimated for values of structure constants Q_i fixed from the bosonization of the NJL-model with reduction of meson resonances. Table 2 shows that the Born contribution at $O(p^6)$ is very small as compared to loop contributions and does not play an essential role in our further analysis of decay

[3]There is no cancellation of the contribution of the electromagnetic penguin operator $\mathcal{O}_8$ at the lowest order and the first terms in the expressions (12) for $\mathcal{A}_{0,2}^{(8)}$ correspond to the contributions at $O(p^0)$.

amplitudes and $\varepsilon^{'}/\varepsilon$.

A strong indication that the development to higher orders is physically sensitive is given by the behaviour of phases: the strong interaction phases $\delta_{2,0}$ arise first at $O(p^4)$, but for the quantitative description of the phases it is necessary to go beyond $O(p^4)$. At $O(p^4)$, for the $\pi\pi$-scattering phase shifts and their difference $\Delta = \delta_0 - \delta_2$, we have obtained the values of $\delta_0 \approx 22^\circ$, $\delta_2 \approx -13^\circ$, $\Delta \approx 35^\circ$ which are in agreement with [32]. At $O(p^6)$, however, we obtained $\delta_0 \approx 35^\circ$, $\delta_2 \approx -9^\circ$, $\Delta \approx 44^\circ$, in a better agreement with the experimental value $\Delta^{exp} = (48 \pm 4)^\circ$ [33].

5 Phenomenological results

In our approach the parameters ξ_i in Eq. (11) are treated as phenomenological (μ-independent) parameters to be fixed from the experimental data. They can be related to the μ-dependent QCD predicted $\xi_i(\mu)$ by using some μ-dependent $\widetilde{B}_i$-factor defined as

$$\xi_i^{ph} = \xi_i(\mu)\widetilde{B}_i(\mu).$$

The factors $\widetilde{B}_i(\mu)$ can be related to the factors $B_i(\mu)$ defined in (2) by obvious relations. Table 3 shows the QCD predictions for the coefficients $\xi_i(\mu) = \xi_i^{(z)}(\mu) + \tau\xi_i^{(y)}(\mu)$ which correspond to the Wilson coefficients

$$c_i(\mu) = z_i(\mu) + \tau y_i(\mu), \quad \tau = -\frac{V_{td}V_{ts}^*}{V_{ud}V_{us}^*},$$

from the table XVIII of Ref. [1] calculated numerically from perturbative QCD at $\mu = 1$ GeV for $m_t = 170$ GeV in leading (LO) and next-to-leading orders in "naive dimensional regularization" (NDR) and $^{'}$t-Hooft-Veltman (HV) regularization schemes. The numerical values of the QCD scale $\Lambda^{(4)}_{\overline{MS}}$ given in table 3 correspond to $\alpha^{(4)}_{\overline{MS}}(M_Z) = 0.119 \pm 0.003$. $\xi_i^{(z)}$ and $\xi_i^{(y)}$ were obtained from z_i and y_i, respectively, using the Eqs. (3) and (5).

As we cannot calculate the factors $\widetilde{B}_i(\mu)$ theoretically, they can be fixed only from data in the spirit of the semi-phenomenological approach [1, 4, 8]. Table 2 shows that the amplitudes of $K \to 2\pi$ decays are dominated by the contribution of the operators $\mathcal{O}_i$ with $i = 1, 2, 3, 4, 5, 8$. Moreover, in case of the operators $\mathcal{O}_{1,2,3}$, the first term in the combination $(-\xi_1 + \xi_2 + \xi_3)$ dominates in the effective weak meson lagrangian (4). Thus, the isotopic amplitudes can be given after restriction to the

dominating contributions of four-quark operators as

$$\begin{aligned}
\mathcal{A}_I &= \mathcal{A}_I^{(z)} + \tau \mathcal{A}_I^{(y)} \,, \\
\mathcal{A}_I^{(z,y)} &= \Big[-\xi_1^{(z,y)}(\mu) + \xi_2^{(z,y)}(\mu) + \xi_3^{(z,y)}(\mu) \Big] \widetilde{B}_1(\mu)\, \mathcal{A}_I^{(1)} + \xi_4^{(z,y)}(\mu) \widetilde{B}_4(\mu)\, \mathcal{A}_I^{(4)} \\
&\quad + \xi_5^{(z,y)}(\mu) \widetilde{B}_5(\mu)\, \mathcal{A}_I^{(5)} + \xi_8^{(z,y)}(\mu) \widetilde{B}_8(\mu)\, \mathcal{A}_I^{(8)} \Big] \,, \qquad (13)
\end{aligned}$$

and the relation (11) to the measurable amplitudes may be modified to

$$A_I = (a_I^{(z)} + \tau a_I^{(y)})\, e^{i\delta_I} \,.$$

At least two factors $\widetilde{B}_1$ and $\widetilde{B}_4$ can be estimated from the experimental values $\mathcal{A}_0^{exp} \approx 10.9$ and $\mathcal{A}_2^{exp} \approx 0.347$ (for fixed $\widetilde{B}_5$ and $\widetilde{B}_8$) while the other two (penguin) factors $\widetilde{B}_5$ and $\widetilde{B}_8$ should be fixed from other data. The factors $\widetilde{B}_1$, $\widetilde{B}_4$, $\widetilde{B}_5$ and $\widetilde{B}_8$ are the analogs of the bag factors $B_2^{(1/2)}$, $B_1^{(3/2)}$, $B_6^{(1/2)}$ and $B_8^{(3/2)}$, respectively, introduced in [1].

The parameter $\varepsilon^{'}$ of direct CP-violation in $K \to 2\pi$ decays can be expressed by the formulae

$$\varepsilon^{'} = -\frac{\omega}{\sqrt{2}} \frac{\mathrm{Im}\, a_0}{\mathrm{Re}\, a_0} (1-\Omega)\, \mathrm{e}^{i(\pi/2+\delta_2-\delta_0)} \,, \quad \omega = \frac{\mathrm{Re}\, a_2}{\mathrm{Re}\, a_0} \,, \quad \Omega = \frac{1}{\omega} \frac{\mathrm{Im}\, a_2}{\mathrm{Im}\, a_0} \,,$$

and the ratio $\varepsilon^{'}/\varepsilon$ be estimated as (recall that, experimentally, $\varepsilon^{'}/\varepsilon \approx \mathrm{Re}\, \varepsilon^{'}/\varepsilon$, $\arg \varepsilon \approx \arg \varepsilon^{'}$)

$$\frac{\varepsilon^{'}}{\varepsilon} = \mathrm{Im}\, \lambda_t\, (P_0 - P_2), \quad P_I = \frac{\omega}{\sqrt{2}\varepsilon |V_{ud}||V_{us}|} \frac{a_I^{(y)}}{a_I^{(z)}} \,, \qquad (14)$$

with $\mathrm{Im}\, \lambda_t = \mathrm{Im}\, V_{ts}^* V_{td} = |V_{ub}||V_{cb}| \mathrm{sin}\delta = \eta |V_{us}||V_{cb}|^2$ in the standard and the Wolfenstein parameterizations of the CKM matrix.

Table 4 gives the estimates of $\varepsilon^{'}/\varepsilon$ from a semi-phenomenological approach obtained after fixing the correction factors $\widetilde{B}_1$ and $\widetilde{B}_4$ for isotopic amplitudes in the representation (13) by experimental (CP-conserving) data on $\mathrm{Re}\, \mathcal{A}_{0,2}$, and setting $\widetilde{B}_5 = \widetilde{B}_8 = 1$. We have used the matrix elements of the operators $\mathcal{O}_i$ displayed in table 2 (for central values of phenomenological structure coefficients L_i given in table 1), and the theoretical values $\xi_i(\mu)$ from table 3. The values $(\varepsilon^{'}/\varepsilon)_{min}$ and $(\varepsilon^{'}/\varepsilon)_{max}$ correspond to the interval for $\mathrm{Im}\, \lambda_t$ obtained from the phenomenological analysis of indirect CP violation in $K \to 2\pi$ decay and $B^0 - \overline{B}^0$ mixing [1, 8]:

$$0.86 \cdot 10^{-4} \le \mathrm{Im}\, \lambda_t \le 1.71 \cdot 10^{-4} \,. \qquad (15)$$

Table 4 demonstrates the modification of the semi-phenomenological estimates of the parameters $\widetilde{B}_1$, $\widetilde{B}_4$ and $(\varepsilon^{'}/\varepsilon)_{max}$ after successive inclusion of the corrections at

$O(p^4)$ and $O(p^6)$. Most important are the corrections at $O(p^4)$. The peculiarity of the results at $O(p^2)$ lies in the observation that all estimates of $\varepsilon^{'}/\varepsilon$ lead to negative values. This is related to the fact that in the case corresponding to table 4a the contribution of gluonic penguins to $\Delta I = 1/2$ transitions appears to be suppressed, leading, after the interplay between gluonic and electromagnetic penguins, to the relation $P_0 < P_2$ for the two competing terms in (14). Generally speaking, $\Delta I = 1/2$ transitions loose importance compared to $\Delta I = 3/2$ when estimating $\varepsilon^{'}/\varepsilon$. The situation already changes after inclusion of the correction at $O(p^4)$, due to relative enhancement of the matrix elements for the operator $\mathcal{O}_5$ (see table 4b). Taking into account the dependence of the Wilson coefficients on the renormalization scheme, after including the corrections at $O(p^4)$ and $O(p^6)$ we obtained the following upper and lower bounds for $\varepsilon^{'}/\varepsilon$ (see table 4c):

$$-\,3.2 \cdot 10^{-4} \leq \varepsilon^{'}/\varepsilon \leq 3.3 \cdot 10^{-4}\,, \tag{16}$$

where the range characterizes the uncertainty from short-distance physics.

Our calculations have shown that especially the penguin matrix elements are most sensitive to various refinements: higher-order derivative terms in chiral lagrangians, the reduction of meson resonances, $\pi^0 - \eta - \eta^{'}$ mixing, and meson loop corrections. It should be added that the modification of penguin matrix elements, discussed in this note, is much more important for gluonic than for electromagnetic penguin transitions. This is obvious from the observation that the latter at the lowest order contain terms of $O(p^0)$ which remain unchanged when taking into account the additional terms derived from the effective lagrangian at $O(p^4)$.

We give some results concerning the dependence of the above semi-phenomenological estimates for $\varepsilon^{'}/\varepsilon$ on the choice of the penguin correction factors $\widetilde{B}_5$ and $\widetilde{B}_8$ (figure 2) and on the values of the structure constants L_i (figure 3). In figure 3 we show the dependencies of $\varepsilon^{'}/\varepsilon$ on the coefficients L_4, L_5 and L_8 only, to demonstrate the appreciable sensitivity to the variation of these parameters within their phenomenological bounds given in table 1. It is caused by the fact, that the coefficients L_4, L_5 and L_8 appear in penguin contributions to the $K \to 2\pi$ amplitudes already at $O(p^2)$ (see (12)) while all other structure coefficients given in table 1 appear in the amplitudes of higher orders.

To study the upper and lower bounds for $\varepsilon^{'}/\varepsilon$ corresponding to the variation of the parameters L_i and $\mathrm{Im}\,\lambda_t$ within their phenomenological bounds, we have used the so called "scanning" and "Gaussian" methods [8]. In the first case the parameters L_i

were scanned independently within the intervals defined by their central values and errors given in table 1 while the parameter $\mathrm{Im}\,\lambda_t$ was scanned within phenomenological bounds (15). In the second case we calculated the probability density distribution for $\varepsilon^{'}/\varepsilon$ obtained by using Gaussian distributions for the parameters L_i with errors given in table 1 [4] while for the parameter $\mathrm{Im}\,\lambda_t$ using the result obtained in [8]:

$$\mathrm{Im}\,\lambda_t = (1.29 \pm 0.22) \cdot 10^{-4}\,.$$

In tables 5 and 6 the "scanning" and "Gaussian" results for $\varepsilon^{'}/\varepsilon$ are given for different values of $\widetilde{B}_5$ ($\widetilde{B}_8 = 1$). Figure 4 shows typical probability density distributions for $\varepsilon^{'}/\varepsilon$ obtained in the Gaussian case.

Our results demonstrate that even after taking into account all uncertainties related to both phenomenological input parameters and renormalization scheme dependence, it is still rather problematic to explain theoretically with $\widetilde{B}_5 = \widetilde{B}_8 = 1$ the value of the direct CP-violation parameter $Re(\varepsilon^{'}/\varepsilon) = (23.0 \pm 6.5) \times 10^{-4}$ measured in the experiment NA31 at CERN [21]. The rather high level of direct CP-violation observed in this experiment was confirmed by recent measurements of KTeV at FNAL [22], $(28.0 \pm 4.1) \times 10^{-4}$, and NA48 at CERN [23], $(18.5 \pm 7.3) \times 10^{-4}$. Taking into account the result of the experiment E731 at FNAL [34], $(7.4 \pm 5.9) \times 10^{-4}$, the world averaged value is estimated as

$$Re(\varepsilon^{'}/\varepsilon) = (21.2 \pm 2.8) \times 10^{-4}\,. \tag{17}$$

Finally, we give some results concerning the factor $\widetilde{B}_5$ required to describe the experimental value (17) within our semi-phenomenological approach. In figures 5, 6 and 7 we show the probability density distribution for factors $\widetilde{B}_1$, $\widetilde{B}_4$ and $\widetilde{B}_5$, respectively, obtained by using Gaussian distributions for the parameters L_i, $\mathrm{Im}\,\lambda_t$ and $\varepsilon^{'}/\varepsilon$. The parameters $\widetilde{B}_1$, $\widetilde{B}_4$ and $\widetilde{B}_5$ were defined from the experimental values of the isotopic $K \to 2\pi$ amplitudes $\mathcal{A}_0$, $\mathcal{A}_2$ and the ratio $\varepsilon^{'}/\varepsilon$ with $\widetilde{B}_8 = 1$. The dispersion of these parameter values in figures 5, 6 and 7 is caused mainly by the uncertainties of L_i and $\mathrm{Im}\lambda_t$, while the experimental error of $\varepsilon^{'}/\varepsilon$ is much less influence. Figure 7 demonstrates the necessity for a rather large factor $\widetilde{B}_5$. It should be emphasized, that for even larger values of $\widetilde{B}_5$, the contribution of nonpenguin operators to the $\Delta I = 1/2$ amplitude are still dominating (see figure 8). In figure 9 the probability density plots show the correlations between parameters $\widetilde{B}_1$, $\widetilde{B}_4$ and

[4] With exception of L_4 which is not determined experimentally and therefore taking uniform distribution inside "theoretical" limits $-0.8 \cdot 10^{-3} \le L_4 \le 0.2 \cdot 10^{-3}$.

$\widetilde{B}_5$. The correlations between pairs of parameters $\widetilde{B}_1$, $\widetilde{B}_4$ and $\widetilde{B}_5$, $\widetilde{B}_4$ are caused by the isotopic symmetry breaking related with $\pi^0 - \eta - \eta^{'}$ mixing. The first plot in figure 9 demonstrates the strong correlation between $\widetilde{B}_1$ and $\widetilde{B}_4$. Due to relatively small contributions of penguin operators to isotopic amplitudes of $K \to \pi\pi$ decays there are no visible correlations between $\widetilde{B}_1$, $\widetilde{B}_5$ and $\widetilde{B}_4$, $\widetilde{B}_5$. Figure 10 shows the correlations between $\widetilde{B}_5$ and $\widetilde{B}_8$ calculated for central values of the phenomenological constants L_i and $\mathrm{Im}\,\lambda_t$ with $\mathrm{Re}(\varepsilon^{'}/\varepsilon) = 21.2 \times 10^{-4}$ used as experimental input. From this figure one can see that even for $\widetilde{B}_8 = 0$ values of $\widetilde{B}_5 > 2$ are necessary to explain the large value of $\varepsilon^{'}/\varepsilon$ (17).

6 Conclusion

From studying the impact of the recently confirmed large $\varepsilon^{'}$ value on the parameterization of the hadronic weak lagrangian, including step by step various refinements, we have shown the necessity for a rather large gluonic penguin contribution (the factor $\widetilde{B}_5$ is found well above 1, see figure 7). The large $\widetilde{B}_1$ and $\widetilde{B}_5$ values may be a hint that the long-distance contributions are still not completely understood. An analogous conclusion has been drawn in [35], where also possible effects from physics beyond the Standard Model are discussed. From the phenomenological point of view, there is no difficulty in taking (4) as a bona-fide weak current-current lagrangian with coupling constants ξ_i to be fixed experimentally. The problems arise when matching these parameters to Wilson coefficients derived from perturbative QCD, which is, of course, a necessary requirement. It should be remarked that in our approach there is also no convincing argument for the large correction factor $\widetilde{B}_1$ (due to the $\Delta I = 1/2$ rule); but then we may ask, why $\widetilde{B}_1$ and $\widetilde{B}_5$ should behave differently: as can be seen from table 2, the relative changes of the respective matrix elements in going to higher powers of p^2 do not differ very much.

In this context, one should note recent progress in the estimates of the B-factors with a matching procedure based on higher-order calculations in the long-distance regime within the $1/N_c$-expansion. An essential enhancement of the bag factor for the gluonic penguin operator by the $1/N_c$ corrections at next-to-leading order in the chiral expansion has been observed in [36], where the value $B_6^{(1/2)} = 1.6 \pm 0.1$ has been obtained. The similar value, $B_6^{(1/2)} = 1.6 \pm 0.3$, arising from $O(p^4)$ chiral loop corrections, was obtained in [10, 11] within the semiphenomenological chiral quark model with values of the quark and gluon condensates fixed by reproducing

the $\Delta I = 1/2$ rule.

Since our results are very sensitive to the relative contribution of the gluonic penguin operator, the question of its phenomenological separation in $K \to 2\pi$ decays becomes critical, in the context of the $\Delta I = 1/2$ rule as well as for a very important problem of direct CP-violation. CP-conserving $K \to 2\pi$ data alone are clearly not sufficient for such a separation. It could be accomplished, on the other hand, when taking into account Dalitz-plot data for $K \to 3\pi$ as well as differential distributions for radiative decays $K \to 2\pi\gamma$, $K \to \pi 2\gamma$ described by the same lagrangian (1). As emphasized above, the reason for this possibility is found in the difference in momentum power counting behavior between penguin and non-penguin matrix elements, which appears in higher orders of the chiral theory, when calculating various parameters of differential distributions, for instance, slope parameters of the Dalitz-plot for $K \to 3\pi$. A substantial improvement in the accuracy of such experimental data (mostly being of older dates) would be very helpful for such a phenomenological improvement of the theoretical situation for ε'/ε (see [25] for discussion of this point and [37, 38] for some recent measurements).

The authors gratefully acknowledge fruitful and helpful discussions with W.A. Bardeen, A.J. Buras, J. Gasser, E.A. Paschos and P.H. Soldan.

References

[1] G.Buchalla, A.J.Buras and M.E.Lautenbacher, Rev. Mod. Phys. 68 (1996) 1125.

[2] A.I.Vainshtein, V.I.Zakharov and M.A.Shifman, JETP 72 (1977) 1275;
M.A.Shifman, A.I.Vainshtein and V.I.Zakharov, Nucl. Phys. B120 (1977) 316.

[3] F.J.Gilman and M.B.Wise, Phys. Rev. D20 (1979) 2392.

[4] G.Buchalla, A.J.Buras and M.K.Harlander, Nucl. Phys. B337 (1990) 313.
A.J.Buras, M.Jamin, M.E.Lautenbacher and P.H.Weisz, Nucl. Phys. B370 (1992) 69; addendum Nucl. Phys. B375 (1992) 501.
A.J.Buras, M.Jamin and M.E.Lautenbacher, Nucl. Phys. B408 (1993) 209.

[5] M.Ciuchini, E.Franko, G.Martinelli and L.Reina, Nucl. Phys. B415 (1994) 403.
M.Ciuchini et al., Z. Phys. C68 (1995) 239.

[6] L.Conti, A.Donini, V.Gimenez, G.Martinelli, M.Talevi and A.Vladikas, Phys.Lett. B421 (1998) 273.

G.Kilcup, R.Gupta and S.R.Sharpe, Phys. Rev. D57 (1998) 1654.
R.Gupta, Preprint LAUR-98-271, hep-ph/9801412.
D.Pekurovsky and G.Kilcup, hep-lat/9812019.
D.Pekurovsky and G.Kilcup, Nucl. Phys. (Proc. Suppl.) 63 (1998) 293.

[7] W.A.Bardeen, A.J.Buras and J.-M.Gérard, Phys. Lett. B192 (1987) 138.

[8] A.J.Buras, M.Jamin and M.E.Lautenbacher, Phys. Lett. B389 (1996) 749.

[9] M.Ciuchini, Nucl. Phys. (Proc. Suppl.) B59 (1997) 149.

[10] S.Bertolini, J.O.Eeg, M.Fabbrichesi and E.I.Lashin Nucl. Phys. B514 (1998) 63, 93.

[11] S.Bertolini, M.Fabbrichesi and J.O.Eeg, hep-ph/9802405.

[12] T.Hambye, G.O.Köhler, E.A.Paschos, P.H.Soldan and W.A.Bardeen, Phys. Rev. D58 (1998) 014017.

[13] S.Weinberg, Physica A96 (1979) 327.

[14] J.Gasser and H.Leutwyler, Nucl. Phys. B250 (1985) 465.

[15] J.Gasser and H.Leutwyler, Ann. Phys. 158 (1984) 142.

[16] J.Bijnens, G.Ecker and J.Gasser, in The Second DAΦNE Physics Handbook, eds. L.Maiani, G.Pancheri, N.Paver, INFN, Frascati, 1995.

[17] Y.Nambu and G.Jona-Lasinio, Phys. Rev. 122 (1961) 345; 124 (1961) 246.

[18] D.Ebert and H.Reinhardt, Nucl. Phys. B271 (1986) 188.

[19] J.Bijnens, C.Bruno and E. de Rafael, Nucl. Phys. B390 (1993) 501.

[20] A.A.Bel'kov and A.V.Lanyov, Phys. Part.Nucl. 29 (1998) 33.

[21] G.D.Barr et al., Phys. Lett. B317 (1993) 233.

[22] A. Alavi-Harati et al., Phys. Rev. Lett. 83 (1999) 22.

[23] Seminar presented by P.Debu for NA48 collaboration, CERN, June 18, 1999; http://www.cern.ch/NA48/FirstResult/slides.html.

[24] J.Bijnens and M.B.Wise, Phys. Lett. B137 (1984) 245.

[25] D.Ebert, A.A.Bel'kov, A.V.Lanyov and A.Schaale, Int. J. Mod. Phys. A8 (1993) 1313.
A.A.Bel'kov, G.Bohm, A.V.Lanyov and A.Schaale, Phys. Part. Nucl. 26 (1995) 239.

[26] M.K.Volkov, Ann. Phys. 49 (1968) 202.

[27] A.A.Bel'kov, A.V.Lanyov and A.Schaale, Acta Physica Slovaca 45 (1995) 135.

[28] A.A.Bel'kov, D.Ebert and V.N.Pervushin, Phys. Lett. B193 (1987) 315;
A.A.Bel'kov, A.V.Lanyov and D.Ebert, Sov. J. Nucl. Phys. 50 (1989) 682;
A.A.Bel'kov, V.N.Pervushin and D.Ebert, Sov. J. Part. Nucl. 22 (1991) 1.

[29] R.S.Chivukula, J.M.Flynn and H.Georgi, Phys. Lett. B171 (1986) 453.

[30] A.A.Bel'kov and A.V.Lanyov, Preprint JINR E11-91-162, Dubna, 1991;
A.V.Lanyov, Proc. of the 6th Joint EPS-APS Int. Conf. on Physics Computing, eds. R.Gruber and M.Tomassini, European Physical Society, Geneva, 1994, p. 179.

[31] S.Bellucci, J.Gasser and M.E.Sainio, Nucl. Phys. B423 (1994) 80; Nucl. Phys. B431 (1994) 413 (E).

[32] J.Kambor, J.Missimer and D.Wyler, Phys. Lett. B261 (1991) 496.

[33] A.A.Bel'kov and V.V.Kostyukhin, Sov. J. Nucl. Phys. 49 (1989) 326.

[34] L.K.Gibbons et al., Phys. Rev. Lett. 70 (1993) 1203.

[35] S.Bosch, A.J.Buras, M.Gorbahn et al., Preprint TUM-HEP-347/99 LMU 06/99, 1999 (hep-ph/9904408).

[36] T.Hambye, G.O.Köhler, E.A.Paschos and P.H.Soldan, Preprint DO-TH 99/10, Dortmund, 1999; hep-ph/9906434.

[37] V.Y.Batusov et al., Nucl.Phys. B516 (1998) 3.

[38] A.Bel'kov et al. Proc. of the 28th Int. Conf. on High Energy Physics, eds. Z.Ajduk and A.K.Wroblewski, World Scientific, vol. 1, p. 1204.
V.Anikeev et al., JINR Rapid Communications 1[87] (1998) 13.

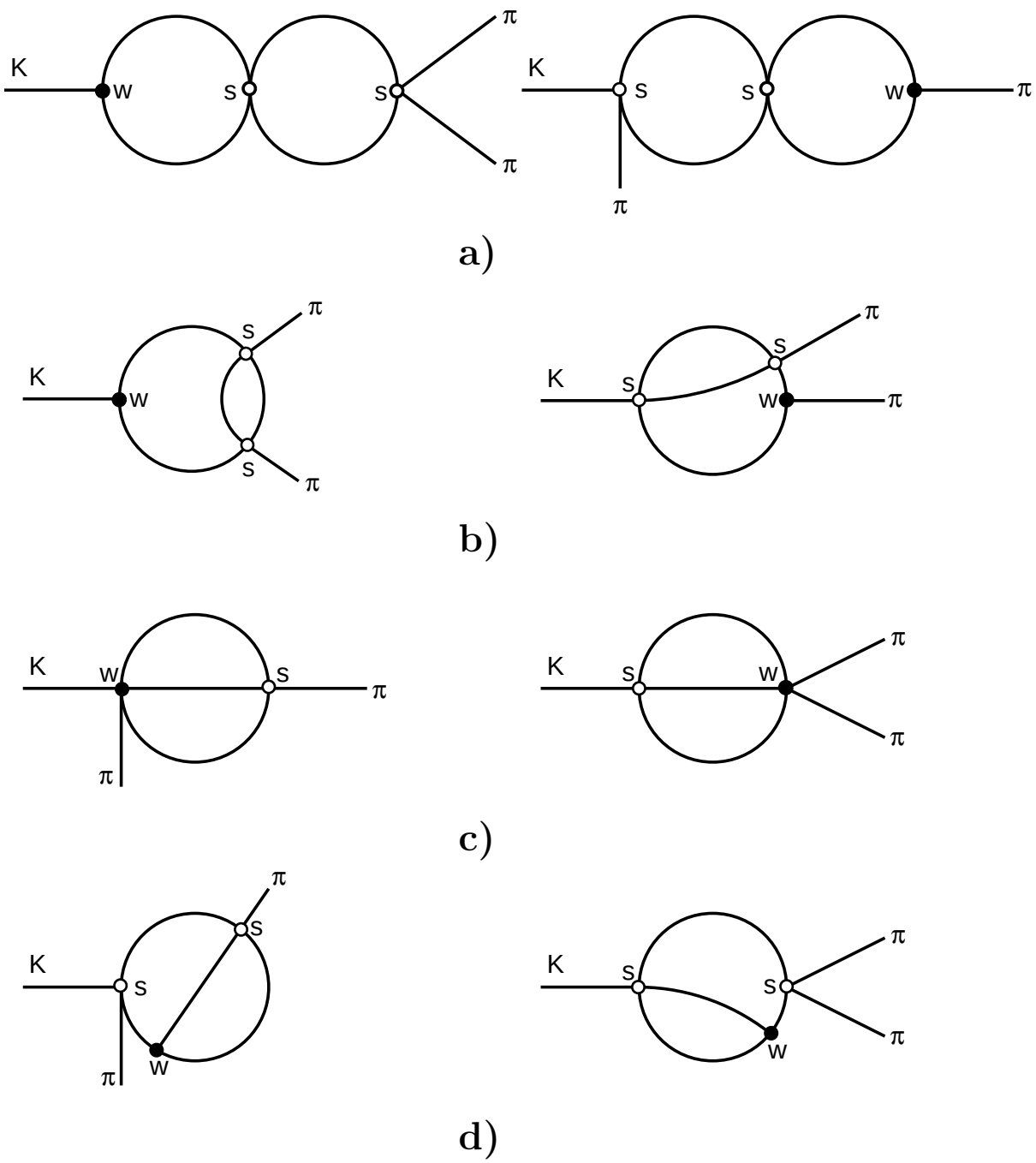

Figure 1. Topology of the main two-loop diagrams at $O(p^6)$ (diagrams with tadpole loops on the external lines and in the vertices are not shown). The external lines denote the momenta. The internal lines correspond to various combinations of virtual pions and kaons in different charge channels. The filled circle denotes the week interaction vertex, the open circle corresponds to strong interaction.

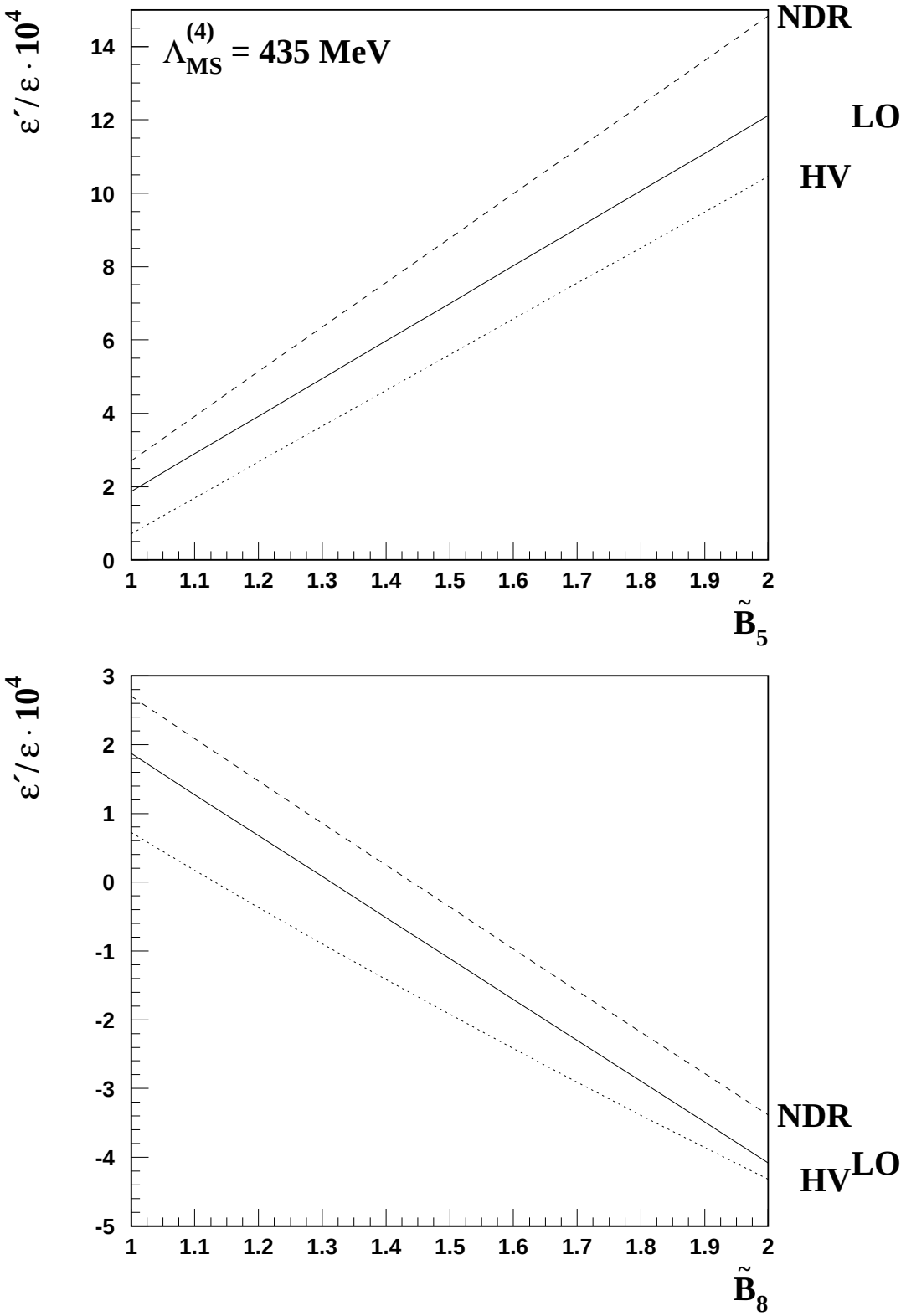

Figure 2. $\widetilde{B}_5$ and $\widetilde{B}_8$-dependence of $\varepsilon^{'}/\varepsilon$ calculated for central values of the phenomenological constants L_i and $\mathrm{Im}\,\lambda_t = 1.29 \cdot 10^{-4}$ with $\Lambda^{(4)}_{\overline{MS}} = 435$ MeV. The $\widetilde{B}_5$-dependence is calculated with $\widetilde{B}_8 = 1$ and the $\widetilde{B}_8$-dependence – with $\widetilde{B}_5 = 1$.

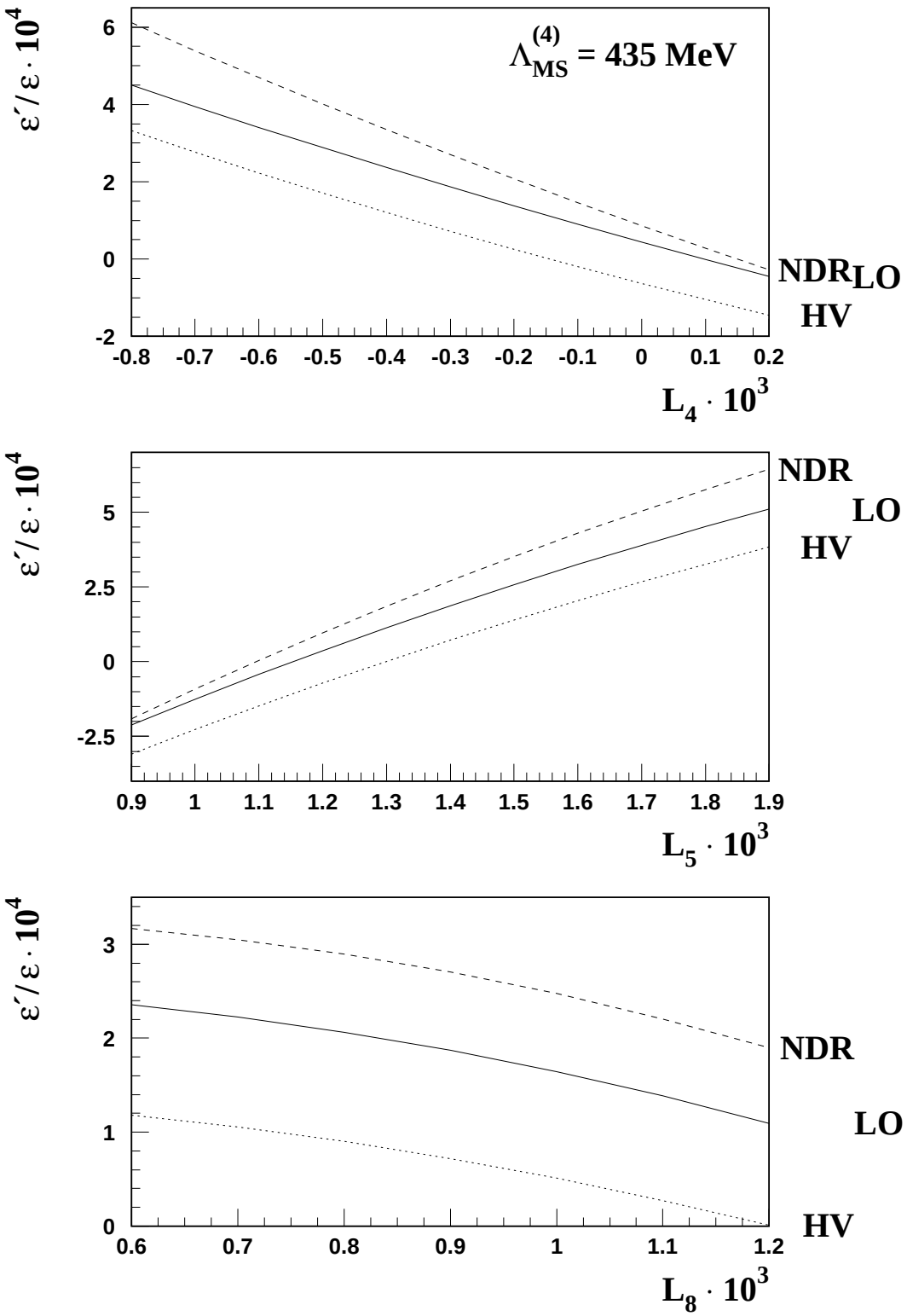

Figure 3. Dependencies of $\varepsilon^{'}/\varepsilon$ on L_4, L_5, and L_8 calculated for central values of Im λ_t and other L_i-coefficients with $\Lambda^{(4)}_{\overline{MS}} = 435$ MeV and $\widetilde{B}_5 = \widetilde{B}_8 = 1$.

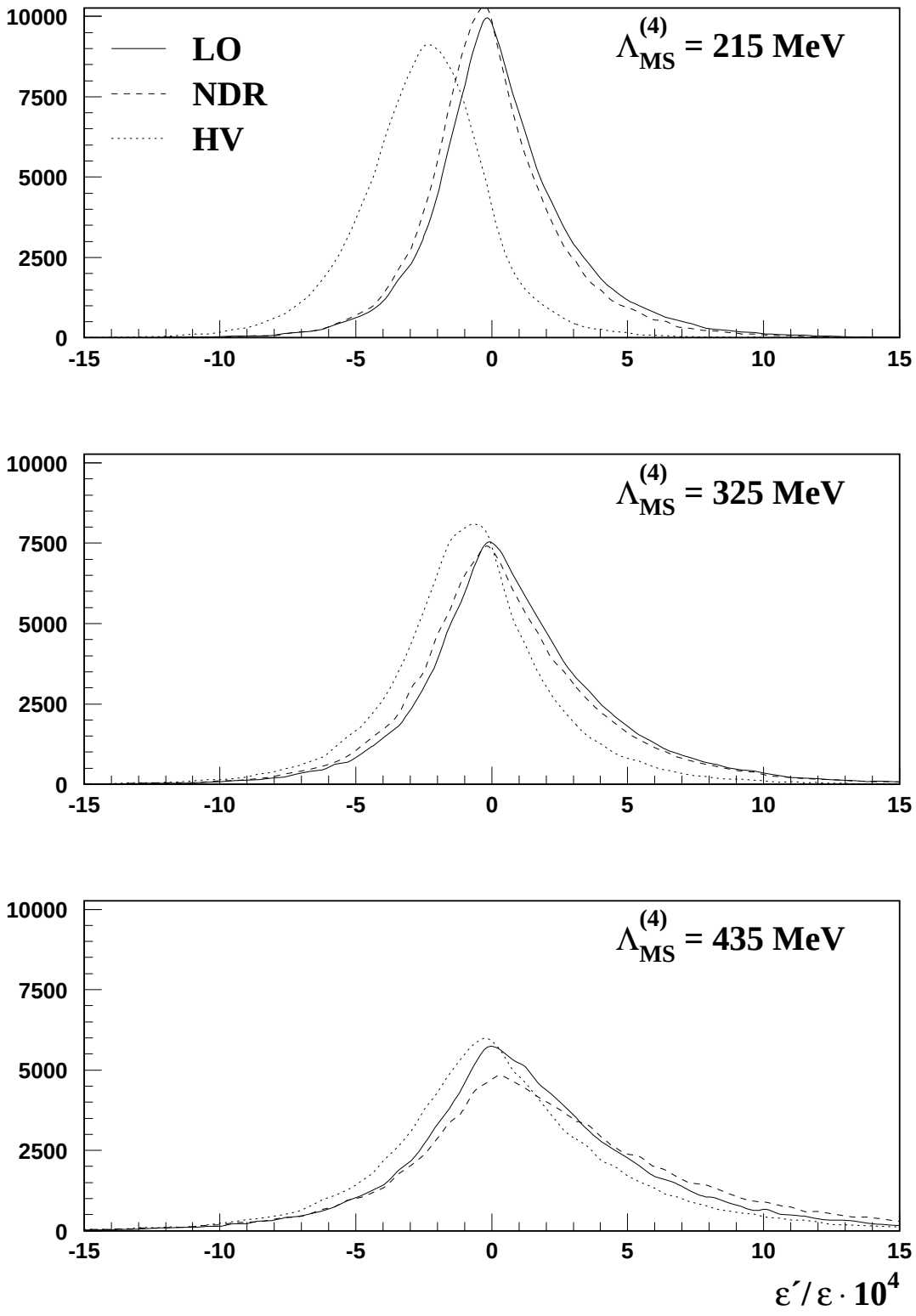

Figure 4. Probability density distributions for $\varepsilon^{'}/\varepsilon$ with $\widetilde{B}_5 = \widetilde{B}_8 = 1$.

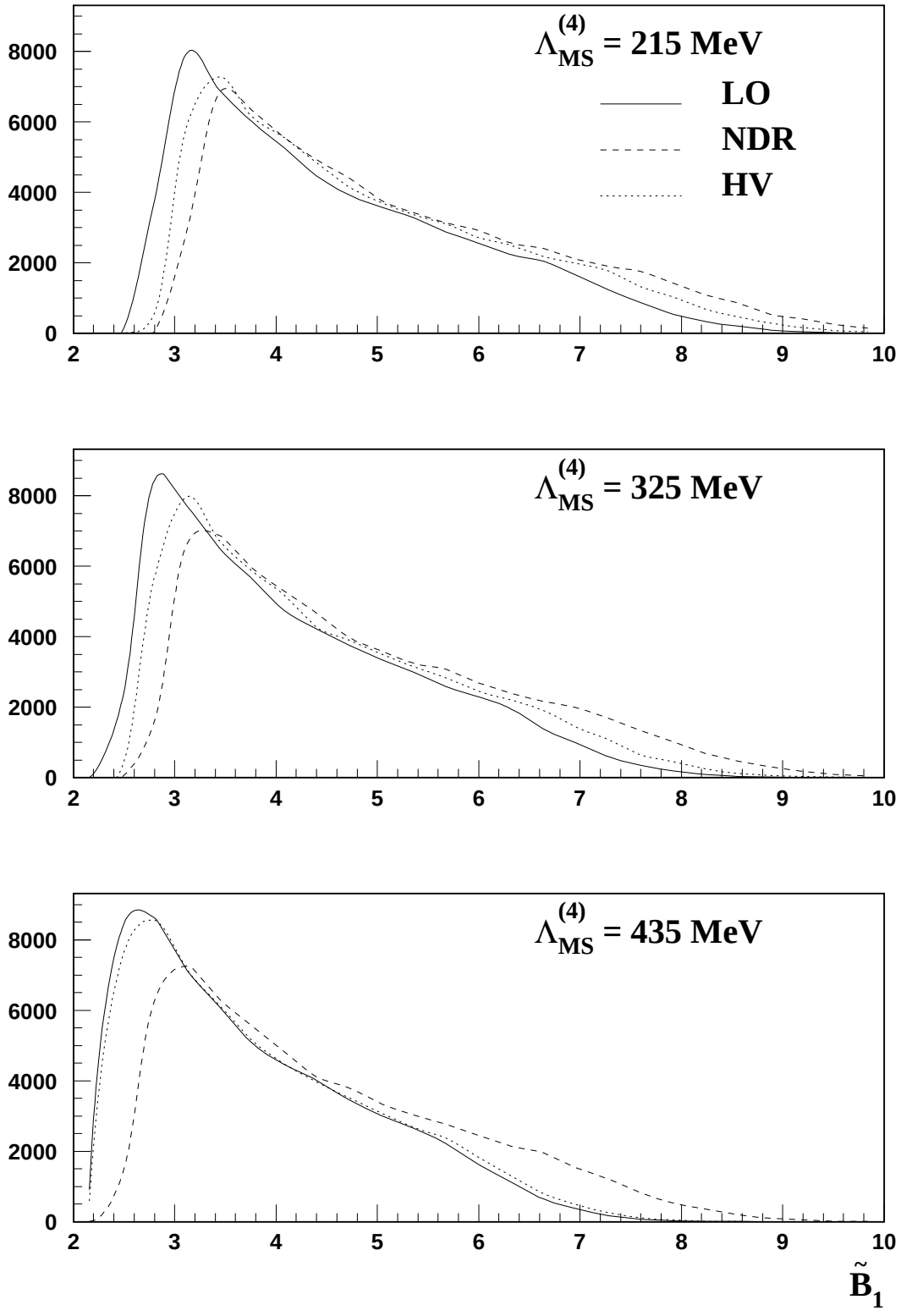

Figure 5. Probability density distributions for $\widetilde{B}_1$ with $\widetilde{B}_8 = 1$.

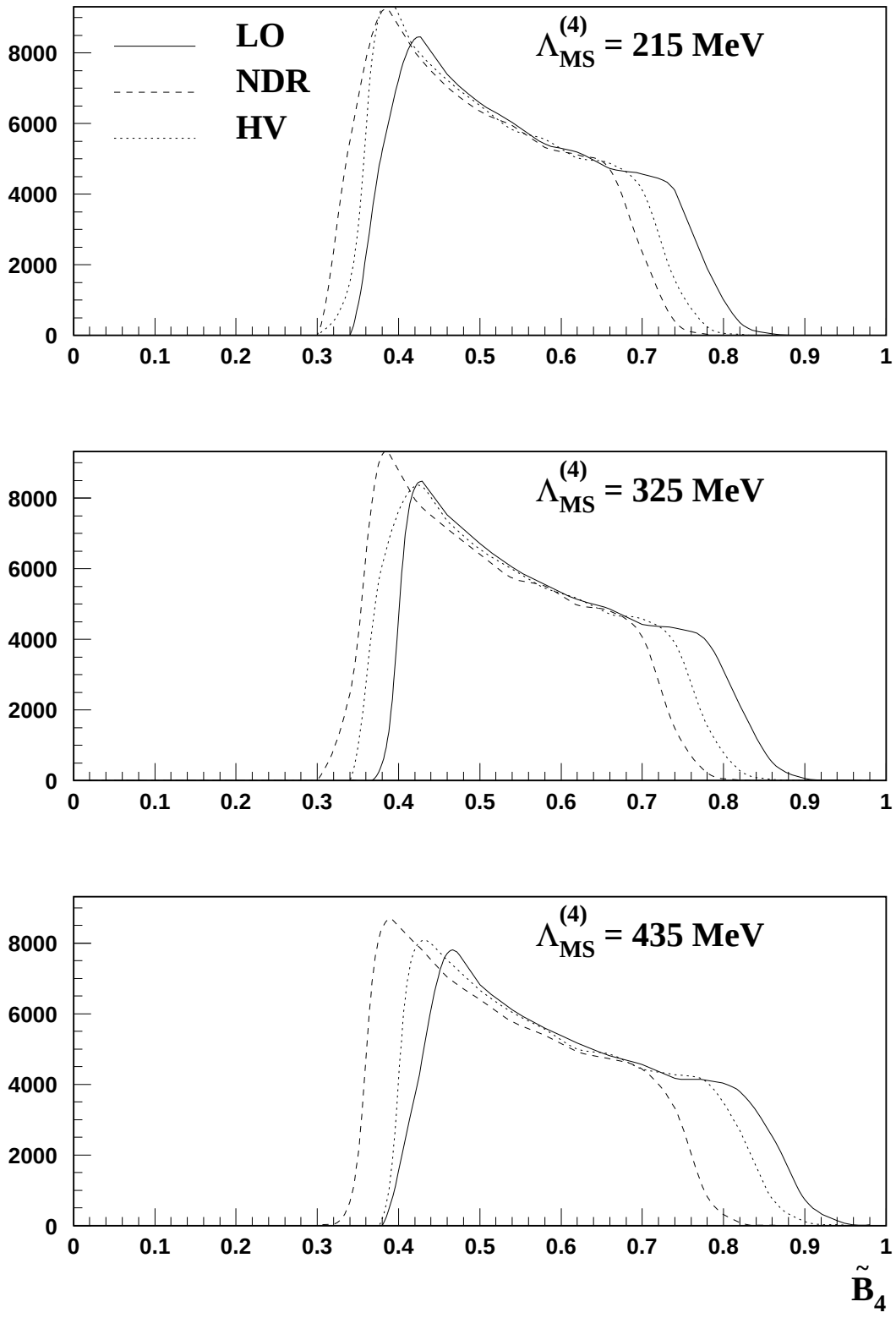

Figure 6. Probability density distributions for $\widetilde{B}_4$ with $\widetilde{B}_8 = 1$.

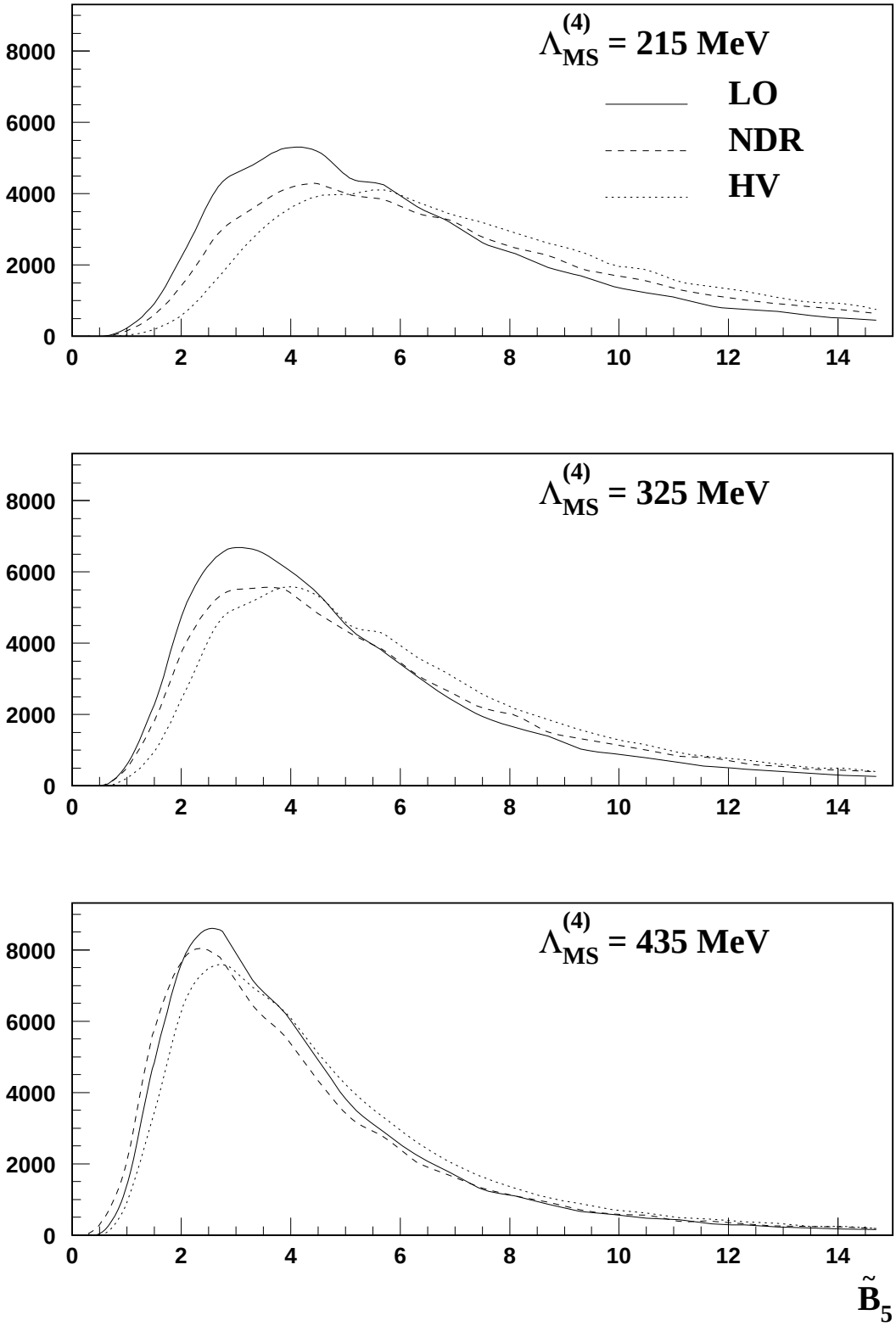

Figure 7. Probability density distributions for $\widetilde{B}_5$ with $\widetilde{B}_8 = 1$.

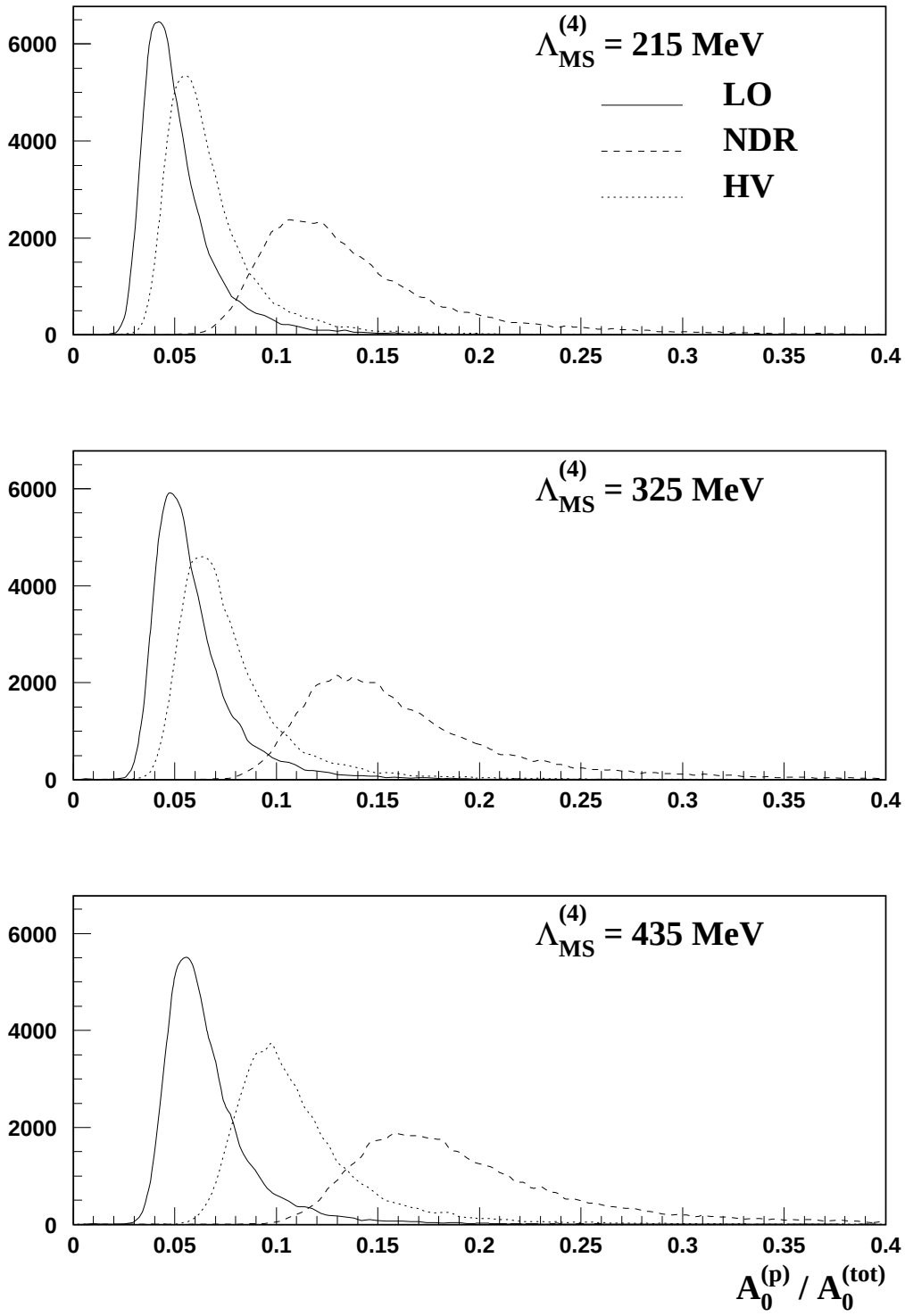

Figure 8. Probability density distributions for the relative contribution of penguin operators to the $\Delta I = 1/2$ amplitude.

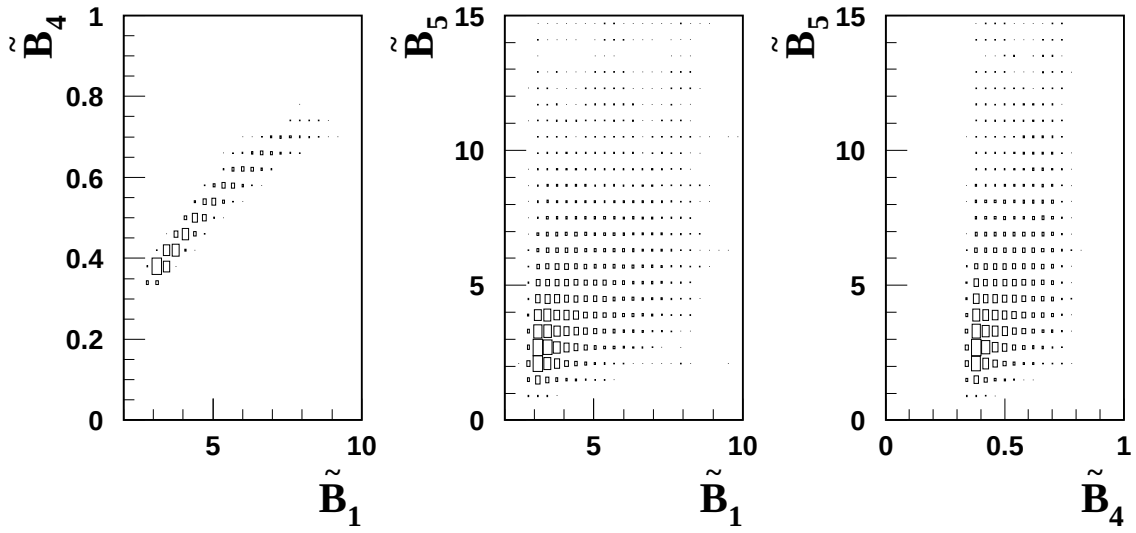

Figure 9. Typical probability density plots for correlations between parameters $\widetilde{B}_1$, $\widetilde{B}_4$ and $\widetilde{B}_5$ calculated with $\widetilde{B}_8 = 1$ and $\Lambda^{(4)}_{\overline{MS}} = 325$ MeV in NDR scheme. For various values of $\Lambda^{(4)}_{\overline{MS}}$ and different renormalization schemes such plots look very similar.

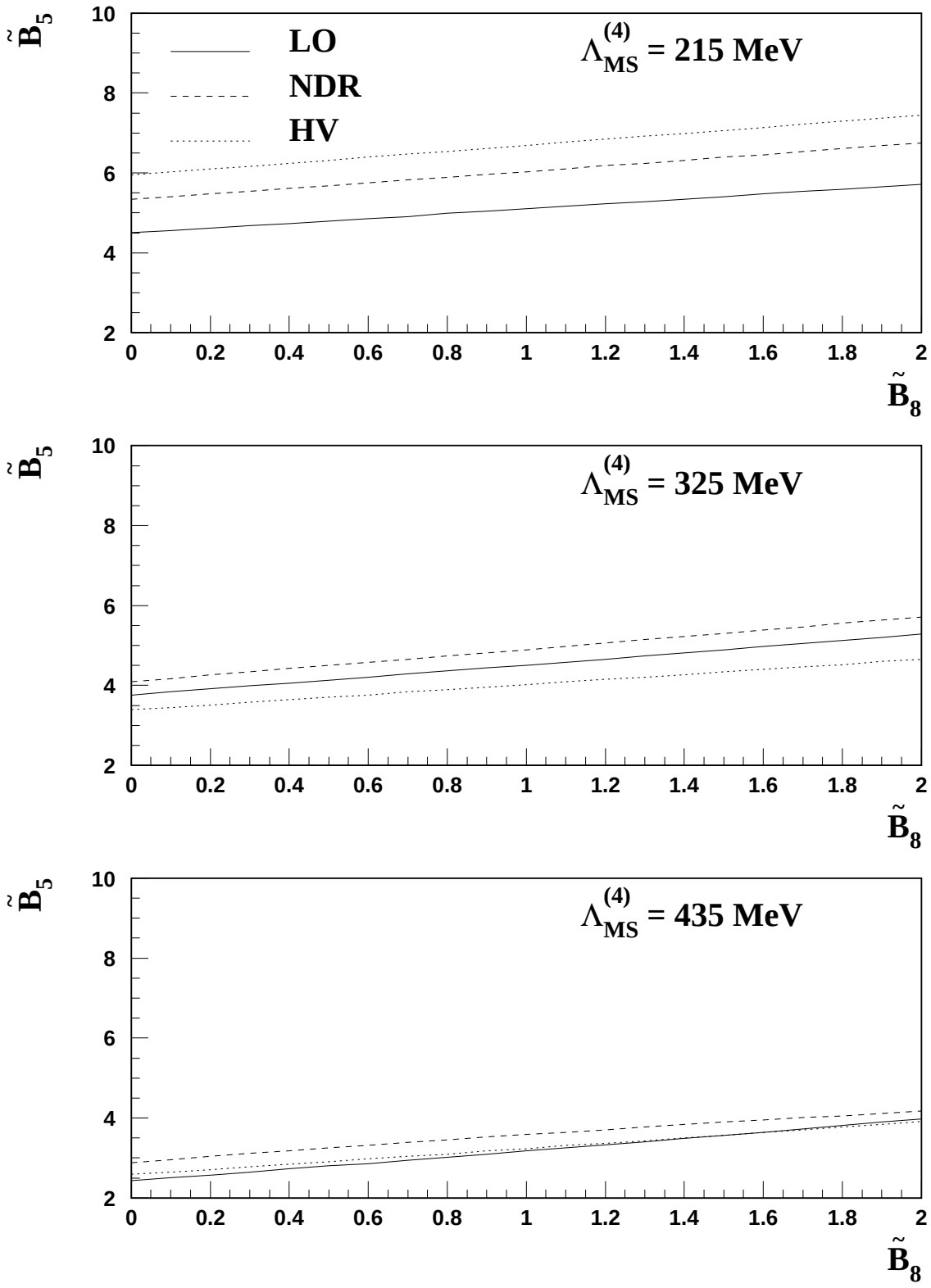

Figure 10. Correlations between parameters $\widetilde{B}_5$ and $\widetilde{B}_8$.

Table 1. Phenomenological and theoretical values of the structure coefficients L_i (in units 10^{-3}).

L_i	Phenomenology [16]			NJL model	
	$L_i^r(m_\rho)$	Input	Γ_i	Without reduction of resonances	After reduction of resonances
1	0.4 ± 0.3	K_{e4} and $\pi\pi \to \pi\pi$	3/32	0.79	0.85
2	1.4 ± 0.3	K_{e4} and $\pi\pi \to \pi\pi$	3/16	1.58	1.70
3	-3.5 ± 1.1	K_{e4} and $\pi\pi \to \pi\pi$	0	-3.17	-4.30
4	-0.3 ± 0.5	$1/N_c$ arguments	1/8	0	0
5	1.4 ± 0.5	F_K/F_π	3/8	0.98	1.64
8	0.9 ± 0.3	$m_{K^0} - m_{K^+}$, L_5, baryon mass ratios	5/48	0.36	1.12

Table 2. Isotopic amplitudes of $K \to 2\pi$ decays

Operators		$\mathcal{O}_1$	$\mathcal{O}_2$	$\mathcal{O}_3$	$\mathcal{O}_4$	$\mathcal{O}_5$	$\mathcal{O}_6$	$\alpha\mathcal{O}_7$	$\alpha\mathcal{O}_8$
	Soft pion approximation								
	$\mathrm{Re}\mathcal{A}_0^{(i)}$	–1.000	1.000	1.000	0.000	–9.623	0.000	0.016	1.458
$O(p^2)$	$\mathrm{Re}\mathcal{A}_2^{(i)}$	0.000	0.000	0.000	1.000	0.000	0.000	–0.016	0.654
	Born diagrams with $\pi_0 - \eta - \eta'$ mixing								
	$\mathrm{Re}\mathcal{A}_0^{(i)}$	0.004	–0.021	–0.039	0.020	0.119	0.004	–0.001	–0.002
	$\mathrm{Re}\mathcal{A}_2^{(i)}$	–0.004	0.021	0.039	–0.002	–0.119	–0.004	0.000	–0.016
Sum	$\mathrm{Re}\mathcal{A}_0^{(i)}$	–0.996	0.979	0.961	0.020	–9.504	0.004	0.015	1.456
p^2	$\mathrm{Re}\mathcal{A}_2^{(i)}$	–0.004	0.021	0.039	0.998	–0.099	–0.004	–0.016	0.638
	Born diagrams								
	$\mathrm{Re}\mathcal{A}_0^{(i)}$	–0.247	0.249	0.236	0.008	–1.626	0.000	0.004	0.037
	$\mathrm{Re}\mathcal{A}_2^{(i)}$	–0.003	0.001	0.015	0.249	–0.059	0.000	–0.004	0.008
$O(p^4)$	1-loop diagrams								
	$\mathrm{Re}\mathcal{A}_0^{(i)}$	–0.171	0.171	0.111	0.001	–2.072	0.000	0.001	0.188
	$\mathrm{Im}\mathcal{A}_0^{(i)}$	–0.482	0.482	0.482	0.000	–4.572	0.000	0.008	0.344
	$\mathrm{Re}\mathcal{A}_2^{(i)}$	0.000	0.000	–0.004	–0.149	0.001	0.000	0.001	–0.006
	$\mathrm{Im}\mathcal{A}_2^{(i)}$	0.000	0.000	0.000	–0.213	–0.004	0.000	0.003	–0.049
	$\mathrm{Re}\mathcal{A}_0^{(i)}$	–1.415	1.399	1.307	0.029	–13.202	0.004	0.020	1.871
Sum	$\mathrm{Im}\mathcal{A}_0^{(i)}$	–0.482	0.482	0.482	0.000	–4.572	0.000	0.008	0.806
$p^2 + p^4$	$\mathrm{Re}\mathcal{A}_2^{(i)}$	–0.007	0.022	0.050	1.099	–0.157	–0.004	–0.018	0.593
	$\mathrm{Im}\mathcal{A}_2^{(i)}$	0.000	0.000	0.000	–0.213	–0.004	0.000	0.003	–0.151
	Born diagrams								
	$\mathrm{Re}\mathcal{A}_0^{(i)}$	–0.003	0.005	0.005	0.000	0.012	0.000	0.000	0.001
	$\mathrm{Re}\mathcal{A}_2^{(i)}$	–0.001	–0.001	–0.001	0.005	–0.004	0.000	0.000	0.000
	1-loop diagrams								
	$\mathrm{Re}\mathcal{A}_0^{(i)}$	–0.106	0.107	0.018	0.002	–0.151	0.000	–0.002	0.016
$O(p^6)$	$\mathrm{Im}\mathcal{A}_0^{(i)}$	–0.229	0.232	0.232	0.000	–1.582	–0.001	0.004	0.063
	$\mathrm{Re}\mathcal{A}_2^{(i)}$	0.000	0.001	0.002	–0.097	–0.004	0.000	0.000	0.007
	$\mathrm{Im}\mathcal{A}_2^{(i)}$	0.000	0.001	0.001	–0.077	–0.001	0.000	0.001	–0.007
	2-loop diagrams								
	$\mathrm{Re}\mathcal{A}_0^{(i)}$	0.202	–0.202	–0.220	0.000	1.753	0.000	–0.003	–0.075
	$\mathrm{Im}\mathcal{A}_0^{(i)}$	–0.169	0.169	0.142	0.000	–1.704	0.000	0.003	0.115
	$\mathrm{Re}\mathcal{A}_2^{(i)}$	0.001	–0.001	–0.001	–0.036	0.000	0.000	0.001	–0.007
	$\mathrm{Im}\mathcal{A}_2^{(i)}$	0.000	0.000	0.000	0.034	0.000	0.000	–0.001	0.006
	$\mathrm{Re}\mathcal{A}_0^{(i)}$	–1.322	1.309	1.111	0.031	–11.588	0.003	0.015	1.664
Sum	$\mathrm{Im}\mathcal{A}_0^{(i)}$	–0.880	0.883	0.856	0.000	–7.858	–0.001	0.014	1.181
$p^2 + p^4 + p^6$	$\mathrm{Re}\mathcal{A}_2^{(i)}$	–0.007	0.021	0.049	0.971	–0.166	–0.004	–0.018	0.566
	$\mathrm{Im}\mathcal{A}_2^{(i)}$	0.000	0.001	0.001	–0.256	–0.003	0.000	0.004	–0.140

Table 3. QCD predictions for the parameters $\xi_i(\mu) = \xi_i^{(z)}(\mu) + \tau\xi_i^{(y)}(\mu)$, calculated with Wilson coefficients $c_i(\mu) = z_i(\mu) + \tau y_i(\mu)$ at $\mu = 1$ GeV for $m_t = 170$ GeV [1].

	$\Lambda^{(4)}_{\overline{MS}} = 215$ MeV			$\Lambda^{(4)}_{\overline{MS}} = 325$ MeV			$\Lambda^{(4)}_{\overline{MS}} = 435$ MeV		
	LO	**NDR**	**HV**	**LO**	**NDR**	**HV**	**LO**	**NDR**	**HV**
$\xi_1^{(z)}$	–1.286	–1.061	–1.165	–1.443	–1.159	–1.325	–1.624	–1.270	–1.562
$\xi_2^{(z)}$	0.187	0.195	0.198	0.172	0.176	0.182	0.157	0.150	0.165
$\xi_3^{(z)}$	0.129	0.143	0.137	0.122	0.137	0.130	0.115	0.131	0.121
$\xi_4^{(z)}$	0.645	0.714	0.687	0.609	0.684	0.650	0.573	0.654	0.599
$\xi_5^{(z)}$	–0.008	–0.020	–0.008	–0.012	–0.032	–0.013	–0.016	–0.056	–0.023
$\xi_6^{(z)}$	0.000	–0.003	0.000	–0.001	–0.007	–0.001	–0.002	–0.021	–0.007
$\xi_7^{(z)}/\alpha$	0.002	0.003	–0.001	0.004	0.008	0.001	0.006	0.015	0.032
$\xi_8^{(z)}/\alpha$	0.000	0.002	0.001	0.001	0.004	0.002	0.001	0.009	0.067
$\xi_1^{(y)}$	0.044	0.038	0.048	0.054	0.048	0.053	0.065	0.060	0.069
$\xi_2^{(y)}$	–0.028	–0.029	–0.030	–0.029	–0.033	–0.030	–0.030	–0.033	–0.030
$\xi_3^{(y)}$	–0.002	–0.002	0.001	–0.002	–0.002	–0.002	–0.002	–0.002	–0.002
$\xi_4^{(y)}$	–0.009	–0.010	0.004	–0.008	–0.009	–0.009	–0.008	–0.009	–0.008
$\xi_5^{(y)}$	–0.081	–0.076	–0.067	–0.109	–0.111	–0.092	–0.143	–0.173	–0.132
$\xi_6^{(y)}$	–0.033	–0.042	–0.021	–0.049	–0.076	–0.033	–0.071	–0.139	–0.051
$\xi_7^{(y)}/\alpha$	0.033	0.004	0.006	0.044	0.013	0.016	0.057	0.027	0.032
$\xi_8^{(y)}/\alpha$	0.031	0.028	0.031	0.043	0.041	0.045	0.058	0.061	0.067

Table 4. Predictions for the parameters of $K \to 2\pi$ decays in the semi-phenomenological approach ($\widetilde{B}_5 = \widetilde{B}_8 = 1$). The ratio $\varepsilon^{'}/\varepsilon$ is given in units 10^{-4}.

a) At $O(p^2)$:

	$\Lambda^{(4)}_{\overline{MS}} = 215$ MeV			$\Lambda^{(4)}_{\overline{MS}} = 325$ MeV			$\Lambda^{(4)}_{\overline{MS}} = 435$ MeV		
	LO	**NDR**	**HV**	**LO**	**NDR**	**HV**	**LO**	**NDR**	**HV**
$\widetilde{B}_1$	6.82	7.74	7.29	6.26	7.27	6.65	5.71	6.76	5.83
$\widetilde{B}_4$	0.54	0.48	0.51	0.57	0.50	0.53	0.60	0.52	0.58
P_0	1.76	1.21	0.59	3.17	2.73	2.06	5.02	5.91	4.29
P_2	2.88	2.49	3.69	4.41	4.20	4.33	6.37	7.03	6.45
$(\varepsilon^{'}/\varepsilon)_{min}$	–0.2	–0.2	–0.5	–0.2	–0.3	–0.4	–0.2	–0.2	–0.4
$(\varepsilon^{'}/\varepsilon)_{max}$	–0.1	–0.1	–0.3	–0.1	–0.1	–0.2	–0.1	–0.1	–0.2

b) Up to and including $O(p^4)$:

	$\Lambda^{(4)}_{\overline{MS}} = 215$ MeV			$\Lambda^{(4)}_{\overline{MS}} = 325$ MeV			$\Lambda^{(4)}_{\overline{MS}} = 435$ MeV		
	LO	**NDR**	**HV**	**LO**	**NDR**	**HV**	**LO**	**NDR**	**HV**
$\widetilde{B}_1$	4.54	5.13	4.85	4.16	4.79	4.42	3.79	4.41	3.86
$\widetilde{B}_4$	0.48	0.43	0.45	0.51	0.48	0.47	0.54	0.46	0.51
P_0	3.94	3.25	2.41	6.09	5.68	4.58	8.87	10.46	7.87
P_2	3.49	3.08	4.20	5.21	5.04	4.99	7.43	8.34	7.34
$(\varepsilon^{'}/\varepsilon)_{min}$	0.4	0.1	–3.1	0.8	0.6	–0.7	1.2	1.8	0.5
$(\varepsilon^{'}/\varepsilon)_{max}$	0.8	0.3	–1.5	1.5	1.1	–0.4	2.5	3.6	0.9

c) Up to and including $O(p^6)$:

	$\Lambda^{(4)}_{\overline{MS}} = 215$ MeV			$\Lambda^{(4)}_{\overline{MS}} = 325$ MeV			$\Lambda^{(4)}_{\overline{MS}} = 435$ MeV		
	LO	**NDR**	**HV**	**LO**	**NDR**	**HV**	**LO**	**NDR**	**HV**
$\widetilde{B}_1$	4.29	4.85	4.58	3.93	4.53	4.17	3.57	4.17	3.64
$\widetilde{B}_4$	0.53	0.48	0.50	0.56	0.50	0.53	0.60	0.51	0.57
P_0	3.93	3.23	2.40	6.08	5.66	4.56	8.87	10.44	7.87
P_2	3.57	3.17	4.29	5.31	5.15	5.07	7.55	8.51	7.43
$(\varepsilon^{'}/\varepsilon)_{min}$	0.3	0.1	–3.2	0.7	0.4	–0.4	1.1	1.7	0.4
$(\varepsilon^{'}/\varepsilon)_{max}$	0.6	0.1	–1.6	1.3	0.9	–0.8	2.2	3.3	0.7

Table 5. Upper and low bounds for $\varepsilon^{'}/\varepsilon$ (in units 10^{-4}) for different values of $\widetilde{B}_5$ ($\widetilde{B}_8 = 1$) obtained by the scanning method.

$\widetilde{B}_5$	$\Lambda^{(4)}_{\overline{MS}}$, (MeV)	LO		NDR		HV	
		min	max	min	max	min	max
1.0	215	-3.8	8.5	-4.0	7.5	-7.2	3.3
	325	-4.5	11.9	-5.1	11.5	-6.6	8.1
	435	-5.5	16.1	-5.9	19.6	-6.6	13.8
1.5	215	-2.4	16.3	-2.7	14.7	-5.6	9.7
	325	-2.6	22.2	-3.1	21.9	-4.1	16.9
	435	-2.9	29.6	-2.9	35.6	-4.2	26.7
2.0	215	-0.9	24.0	-1.3	22.0	-4.4	16.2
	325	-0.7	32.5	-1.2	32.3	-2.5	25.7
	435	-0.4	43.2	0.1	51.4	-1.8	39.5

Table 6. Upper and low bounds for $\varepsilon^{'}/\varepsilon$ (in units 10^{-4}) for different values of $\widetilde{B}_5$ ($\widetilde{B}_8 = 1$) obtained by Gaussian method. The limits without brackets correspond to the confidence level of 68% while the limits in brackets correspond to the confidence level 95%.

$\widetilde{B}_5$	$\Lambda^{(4)}_{\overline{MS}}$, (MeV)	LO		NDR		HV	
		min	max	min	max	min	max
1.0	215	-2.1	3.0	-2.4	2.4	-4.9	-0.2
		(-5.1	7.2)	(-5.1	6.4)	(-8.0	2.6)
	325	-2.3	4.3	-2.7	4.0	-3.6	2.1
		(-6.3	9.9)	(-6.6	9.7)	(-7.6	6.5)
	435	-2.6	5.9	-2.5	7.6	-3.5	4.7
		(-7.8	13.4)	(-8.1	16.6)	(-8.5	11.7)
1.5	215	-0.5	7.3	-0.8	6.5	-3.2	3.1
		(-3.8	14.4)	(-3.9	13.0)	(-6.7	8.3)
	325	-0.2	10.1	-0.5	9.8	-1.5	6.9
		(-4.6	19.5)	(-4.9	19.3)	(-5.9	14.4)
	435	-3.8	14.4	-3.9	13.0	-6.7	8.3
		(-5.5	25.8)	(-5.7	30.8)	(-6.3	23.6)
2.0	215	0.8	11.8	0.5	10.6	-1.8	6.6
		(-2.9	21.8)	(-3.1	20.0)	(-5.7	14.4)
	325	1.5	16.0	1.2	15.8	0.1	11.9
		(-3.4	29.1)	(-3.8	28.9)	(-4.7	22.8)
	435	2.4	21.0	3.2	24.9	1.4	19.1
		(-4.0	36.5)	(-4.0	40.7)	(-4.8	34.5)